

Optical response of a misaligned and suspended Fabry-Perot cavity

G. Cella¹, A. Di Virgilio¹, P. La Penna^{1,2}

¹ *INFN, sez. Pisa*

² *EGO European Gravitational Observatory*

V. D'Auria¹, A. Porzio^{2,3}, I. Ricciardi^{1,4}, S. Solimeno^{1,3,4}

¹ *Dip. Scienze Fisiche, Univ. Federico II*

² *"Coherentia", CNR-INFN, Napoli*

³ *CNISM, Unitá di Napoli*

⁴ *INFN, sez. Napoli*

(Dated: August 6, 2018)

The response to a probe laser beam of a suspended, misaligned and detuned optical cavity is examined. A five degree of freedom model of the fluctuations of the longitudinal and transverse mirror coordinates is presented. Classical and quantum mechanical effects of radiation pressure are studied with the help of the optical stiffness coefficients and the signals provided by an FM sideband technique and a quadrant detector, for generic values of the product $\varpi\tau$ of the fluctuation frequency times the cavity round trip. A simplified version is presented for the case of small misalignments. Mechanical stability, mirror position entanglement and ponderomotive squeezing are accommodated in this model. Numerical plots refer to cavities under test at the so-called Pisa LF facility.

I. INTRODUCTION AND NOTATION

Optical cavities are generally studied by assuming a single mode excitation and ignoring the photon scattering by mirror reflections into other modes. A single mode description is no more reliable when a slight misalignment is sufficient to excite different modes. This situation is met in almost concentric or plane-parallel or confocal configurations. In other cases the weak amplitudes of modes falling outside the resonance bandwidth are of interest. For example, the sensitivity of interferometers with cavities placed in their arms depends on the contribution of higher modes as well as the error signals used for longitudinal and angular alignments.

Optical cavities are generally stabilized, in length, by the Drever-Pound (D-P) technique [1] working with odd harmonics of the phase modulated laser beam.

In order to deal with a large variety of situations the model discussed in this paper accounts for misalignment, detuning and a generic spectrum of harmonics. Faced with the possibility of working with approximate expressions it has been preferred to simplify exact solutions at the end of the calculation. This option avoids difficulty of making adequate approximations in presence of a large number of parameters.

This strategy can be useful for the design studies necessary for the development of future gravitational antennas. It gives the possibility to investigate noise contributions coming from all optical and mechanical degrees of freedom. It can be also used for studying instabilities, optical spring effect, entanglement and radiative pressure squeezing associated to both axial and angular fluctuations for any degree of detuning, misalignment and mismatch.

The present work grew up from the study of short and large spot size resonators [2] implemented at LFF (Low Frequency Facility [3]) a facility dedicated to test-

ing new mechanical suspensions, controls and mirrors for the VIRGO interferometric gravitational antenna, and studying the effects of radiation pressure, mirror and suspensions thermal noise.

Main features of the LFF are the use of suspended mirrors and the possibility of confining large section cavity modes. The mirrors hang from multipendula which guarantee a drastic reduction of the seismic noise above the resonance frequencies of the mechanical modes. The phase-modulated light reflected by the cavity is used by a Pound-Drever apparatus [1] both for stabilizing the cavity length, and measuring the noise spectrum. Several papers analyzed the dynamic and the alignment of cavities sharing some of the LFF features [4, 5, 6]. Numerous specialized studies have been produced by research groups of VIRGO, LIGO, TAMA and GEO projects [7].

Suspended cavities have been analyzed by several authors in different contexts, all sharing the common feature of using a system of Langevin equations for both the mechanical and electromagnetic modes. The coupling of cavity and mechanical modes is represented by suitable potentials [8, 9] leading to a complex interplay between cavity mode amplitudes, mirror positions and orientation fluctuations. In this paper the resonator is regarded as a mechanical Langevin system driven by thermal sources and shot noise. This is done by-passing the Hamiltonian approach and hiding the optical modes fluctuations into the mechanical ones by generalizing an approach introduced in [10]. So doing, the Langevin system contains ponderomotive terms, connected with the classical part of the laser beam and the shot noise. The seismic noise affecting the mechanical system has been neglected. Once known, its local spectral density can be easily added to the thermal one.

Thermal motion of mechanical oscillators has been modelled as standard Brownian motion [11], possibly corrected by Diosi for preserving the quantum mechanical

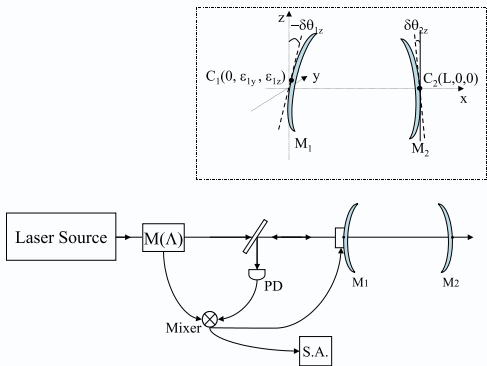


FIG. 1: Typical optical layout of the apparatus examined in the present paper. The laser beam is phase modulated at frequency Λ by the modulator $M(\Lambda)$. The modulated beam drives the cavity. The front M_1 and back M_2 mirrors are suspended to multipendulum chains. The beam reflected by the front mirror is sent to a photodetector PD , and the photodetection signal is demodulated before going to a spectrum analyzer. The same signal is sent to a control system (not shown) which provides a feedback signal applied to mirror M_1 . The noise of the system is studied by spectral analysis.

commutation relations [12], or by non-Lindblad master equations (ME) [13, 14]. Accordingly, in the present model different thermal correlation functions have been introduced.

The quantum field fluctuations (shot-noise) are accounted for by splitting each mode amplitude in a classical and a quantum parts [9, 15] and relying on the input-output theory [16].

Radiation pressure can lead to mechanical instabilities, as predicted by Braginsky and Manukin [17]. Acting on the suspended mirrors it provides a spring action which either depresses or reinforces any perturbation [10, 18, 19, 20]. It may also be used to mechanically entangle the two mirrors [21] or to enhance the squeezing of the output field [22].

In Fig.1 it is represented the typical optical layout of the apparatus that will be examined. Main features of the present model are: i) the multimode description of the cavity field; ii) the inclusion of radiation pressure and shot noise terms; iii) the description of suspensions and mirrors in terms of mechanical modes.

Here and in the following $J = 1, 2$ labels the mirror, x the axial and $q = y, z$ the transverse coordinates. The analysis is focused on the fluctuations of the J 's mirror orientation ($\delta\theta_{Jq}$) and displacements ($\delta x_J, \delta\varepsilon_{Jq}$), combined in the parameters

$$\begin{aligned} \delta\psi_J &= (-1)^J 2k^\ell \delta x_J \\ \delta\alpha_{Jq} &= i(-1)^J \sqrt{2}k^\ell w_J \left(\delta\theta_{Jq} - \frac{\delta\varepsilon_{Jq}}{R_J} \right) \end{aligned} \quad (1)$$

with k^ℓ laser wavenumber, w_J spot size, R_J mirror curvature radius and $\delta\theta_{Jq} = (\delta\vec{\Omega}_J \times \hat{x}) \cdot \vec{q}$ depending on the

rotation's angles $\delta\vec{\Omega}_J$. In addition the mirror vibrations are accounted for by introducing matrices ς_{Js} and functions $\delta\varsigma_{Js}$ representing respectively profile and amplitude of the s -th vibrational mode of the J -th mirror.

The radiation pressure force and torques are linearized with respect to the set $\{\delta\alpha_{Jq}\}$ of transverse mirror coordinates by introducing optical stiffness coefficients. Hence, the Fourier transforms $\{\delta\tilde{\alpha}_{Jq}\}$ satisfy Langevin equations with driving forces proportional to these quantities. They become important in proximity of the suspensions and mirror mechanical resonances. These stiffness coefficients are in general frequency dependent for the presence of the phase factor $e^{i\omega\tau}$, with τ the cavity round trip.

A vector approach has been adopted by representing the amplitudes of the excited cavity modes by a column vector \mathbf{a} while the mismatch and misalignment of the input beam is accounted for by a vector \mathbf{v} . The various quantities O used for describing the system dynamics (e.g. the force acting on a given suspension mode) have been expressed in forms like $O = \mathbf{v}^\dagger \cdot \mathbf{O} \cdot \mathbf{v}$ with \mathbf{O} a matrix representation of the quantity itself. In analogy with quantum mechanics \mathbf{O} is seen as the matrix representation of an operator \hat{O} corresponding to the quantity of interest, and \mathbf{v} as the quantum state of the resonator.

For evaluating spectral densities it has been introduced the symbol \ddagger which is defined by its action on frequency dependent quantities:

$$f^\ddagger(\omega) \equiv f^*(-\omega^*),$$

and the shorthands

$$\begin{aligned} \Im\{f(\omega)\} &= \frac{1}{2i}(f(\omega) - f^\ddagger(\omega)) \\ \Re\{f(\omega)\} &= \frac{1}{2}(f(\omega) + f^\ddagger(\omega)). \end{aligned}$$

The same \ddagger applied to a frequency dependent matrix transforms $\mathbf{O}(\omega)$ into $\mathbf{O}^\ddagger(\omega) = \mathbf{O}^\dagger(-\omega^*)$.

The summation symbol is omitted when applied to expressions containing a repeated index.

The paper is organized in seven sections. Section II is dedicated to the optical modes excited in a cavity with moving mirrors, and to the susceptibilities relative to the noise sources of the suspensions, mirror vibrations and shot noise. The dynamic of the mechanical components (mirrors and suspensions) is discussed in Sec. III while the Drever-Pound and quadrant detector signals are analyzed in Sec. IV.

The results obtained in these sections are combined in Sec. V where a five degrees of freedom model of the cavity, including radiative pressure and torques, is presented. The model is linearized for small misalignments and resonance enhanced effects are discussed in Sec VI where the cavity is examined as a bipartite system. In this context ponderomotive squeezing of the output field and entanglement of two mirror modes are discussed. The manuscript is completed by six mathematical appendices.

The first three of them give the expressions for the stiffness and the Drever-Pound signal matrices together with their simplified expressions in case of small misalignment and mismatch. The last ones are dedicated to thermal and shot-noise sources, and their mutual correlations.

II. CAVITY FIELD

A suspended cavity of length L excited by a time harmonic field is described by a superposition of Hermite-Gauss modes $u_\lambda(\vec{r}, x)$

$$e^{-i\omega^\ell t} \sum_{\sigma=\pm} \exp\left[i\sigma k^\ell \frac{r^2}{2R(x)}\right] a_\lambda^{(\sigma)}(x, t) u_\lambda(\vec{r}, x) .$$

with ω^ℓ the laser frequency, $\sigma = +$ for a wave traveling from mirror 1 toward 2 and $-$ contrariwise. The wavefront curvature $R(x)$ is matched to the mirror's curvature: $R(0) = R_1 < 0$, $R(L) = R_2 > 0$. Each mode is labeled as usual by a couple of integer numbers $(\lambda_y, \lambda_z) \equiv \lambda$. Here and in the following x stands for the optical axis coordinate and $(y, z) \equiv \vec{r}$ are the two transverse ones. Each mode u_λ is taken with a fixed normalization on the transverse section and without phase factors,

$$u_\lambda(\vec{r}) = u_{\lambda_y}(y)u_{\lambda_z}(z) ,$$

while the amplitudes are written as

$$a_\lambda^{(\sigma)}(x, t) = e^{i\sigma[k^\ell x - (\lambda_y + \lambda_z + 1)\phi(x)]} \left| a_\lambda^{(\sigma)}(x, t) \right|$$

where $\phi(x) = \arctan\left(\frac{x-x_0}{b}\right)$ is the phase delay of the Gaussian fundamental mode with respect to a plane wave, x_0 being the distance of the waist from the input mirror and b the confocal parameter. The field is propagated outside the resonator by passing through the different optical components met on the way toward the laser source and the photodetector which provides the error signal.

The laser beam incident on (input) mirror 1 has been split it in a classical and in a quantum term:

$$E^{in}(\vec{r}, t) = e^{-i\omega^\ell t} E (1 + \mu^\ell(t)) u^{in}(\vec{r}) + \delta\hat{a}^{SN} \quad (2)$$

being

$$E = \sqrt{\frac{P}{\hbar\omega^\ell}} = 2.5 \times 10^9 \left(\frac{P}{1W}\right)^{1/2} \left(\frac{\lambda^\ell}{1\mu}\right)^{1/2} \text{ Hz}^{1/2}$$

the mean amplitude, and μ^ℓ the relative amplitude fluctuations. Effects of the laser linewidths have been ignored.

Misalignment and mismatch effects between the input beam and the cavity are taken into account by writing $u^{in}(\vec{r})$ as a superposition of cavity modes, namely

$$u^{in}(\vec{r}) = v_\lambda u_\lambda(\vec{r}) . \quad (3)$$

The structure of the expansion coefficients is factorized in a product of Hermite polynomials

$$v_\lambda \propto \frac{\delta_y \delta_z H_{\lambda_y}\left(v_y \frac{\delta_y^2 - 1}{\delta_y \sqrt{2}}\right) H_{\lambda_z}\left(v_z \frac{\delta_z^2 - 1}{\delta_z \sqrt{2}}\right)}{\sqrt{2^{\lambda_y + \lambda_z} \lambda_y! \lambda_z!}} \quad (4)$$

depending on the misalignment v_q and mismatch δ_q parameters defined respectively by

$$v_q = -i \frac{k^\ell w_1}{\sqrt{2}} \left(\theta_q - \frac{\varepsilon_q}{Q_q} \right)$$

$$\delta_q = \sqrt{1 + i \frac{2}{k^\ell w_1^2} \frac{Q_q Q_1^*}{(Q_q - Q_1^*)}} .$$

For a perfect matching $v = 0$ and $\delta = 0$. Here Q_1 is the complex curvature radius of the cavity mode evaluated at the input mirror, while Q_q , θ_q and ε_q stand for the curvature radius, angular and transverse misalignment of the input beam.

The modal expansion (3) will be used in the following for representing the cavity fields in correspondence of the two mirrors as column vectors \mathbf{v} with components v_λ . So doing the multiplication of $u(\vec{r})$ by a function $w(\vec{r})$ will be represented by the product $\mathbf{w} \cdot \mathbf{v}$ of \mathbf{v} by a matrix \mathbf{w} .

The coupling of the cavity with the universe modes through the partially transmitting mirrors introduces the quantum noise contribution $\delta\hat{a}^{SN}(\mathbf{r}, t)$ of Eq. (2)

$$[\delta\hat{a}^{SN}(\mathbf{r}, t), \delta\hat{a}^{SN\dagger}(\mathbf{r}', t')] = \delta^{(3)}(\mathbf{r} - \mathbf{r}') \delta(t - t')$$

It can be expanded as a superposition of delta-correlated operators $\delta\hat{a}_\lambda^{SN}(t)$,

$$\delta\hat{a}^{SN}(\mathbf{r}, t) = \delta\hat{a}_\lambda^{SN}(t) u_\lambda(\mathbf{r}) . \quad (5)$$

Before arriving at the mirror the excitation beam is passed through a phase modulator represented by the phase factor

$$F = e^{iM \sin(\Lambda t)} = e^{-ip\Lambda t} J_p(M) \quad (6)$$

with $J_p(M)$ the p -th Bessel function of argument M . The input modulation F modifies the laser excited amplitude a_λ^ℓ into a sum of harmonics varying on the time scale of the suspension fluctuations,

$$a_\lambda = J_p e^{-ip\Lambda t} a_{\lambda p} \quad (7)$$

while leaving the noise unaffected.

A. Cavity fluctuations

Owing to the fluctuations of the suspensions the mirror orientations change slowly in time by undergoing torsions $\delta\Omega_{Jz}(t)$, tiltings $\delta\Omega_{Jy}(t)$ and transverse displacements $\delta\vec{\varepsilon}_J(t)$. The mirror can rotate also around the optical axis, but this motion is uncoupled to the cavity field in the linear approximation.

The mirror motions separate into fluctuating and average components, the latter ones setting the reference frame for the vector representation. So doing the average misalignment and displacements will be included in those relative to the input beam, which will be represented by a unit amplitude vector \mathbf{v}_J

$$\mathbf{v}_1 = \mathbf{v}, \quad \mathbf{v}_2 = \mathbf{\Phi}^{\frac{1}{2}} \cdot \mathbf{v}$$

with $\mathbf{\Phi}$ a diagonal matrix of components $\Phi_\lambda = e^{-i2(\lambda_y + \lambda_z + 1)\phi_G}$ and $\phi_G = \phi(L) - \phi(0)$ the single-trip phase delay of the Gaussian fundamental mode. Accordingly in the following the parameters $\delta\alpha_{Jq}$ (see Eq. (1)) will be small fluctuating quantities.

The reflection at mirror 1 induces the transformation $u_\lambda a_\lambda^{(-)} = \mathbf{r}_1 u_\lambda a_\lambda^{(+)}$ with $\mathbf{r}_1(t)$ the phase factor

$$\mathbf{r}_1 = r_1 \exp \left[-ik^\ell \frac{\delta\varepsilon_1^2}{R_1} - i2k^\ell \delta x_1 - i2k^\ell \delta u_1^{DEF} + i2k^\ell \left(\delta\vec{\Omega}_1 \times \hat{x} - \frac{\delta\vec{\varepsilon}_1}{R_1} \right) \cdot \vec{r} \right]. \quad (8)$$

Here $\delta x_1(t)$ is the deviation of the center from the positions at rest ($x_1(t) = 0 + \delta x_1(t)$). $\delta u_1^{DEF}(\vec{r}, t)$ is the tiny deformation of the mirror surface represented by the matrix $\delta\varsigma_1(t)$ of components

$$\delta\varsigma_{1\lambda\lambda'}(t) = 2k^\ell \int u_\lambda(\vec{r}) \delta u_1^{DEF}(\vec{r}, t) u_{\lambda'}(\vec{r}) d^2\vec{r} \quad (9)$$

Expanding further δu_1^{DEF} into mirror modes [23, 24] $\delta\varsigma_1(t)$ becomes a superposition

$$\delta\varsigma_1(t) = \delta\varsigma_{1s}(t) \varsigma_{1s} \quad (10)$$

of matrices ς_{1s} times fluctuating amplitudes $\delta\varsigma_{1s}(t)$ driven by radiation pressure and thermal noise.

Although the frequencies of the mirror acoustic modes are very large, the tails of their spectra contribute to the low frequency thermal noise of the interferometers as recently reported by [25]. Levin [26] has approximated, at very low frequency, the many mode profiles with the steady-state mirror surface deformation $\delta u_1^{DEF}(\vec{r})$ (in matrix form ς_1^L) under the action of the incident beam (positive for a compression), by replacing Eq.(10) with

$$\delta\varsigma_1(t) = \varsigma_1^L \delta\varsigma_1^L(t) \quad (11)$$

$\delta\varsigma_1^L(t)$ being a stochastic process, (see Eq.(43)).

Accordingly, ignoring the quadratic expression $k^\ell \delta\varepsilon_1^2/R_1$ the phase factor \mathbf{r}_1 (Eq.(8)) is represented in vector form by

$$r_1 e^{-i(2k^\ell \delta x_1 + \delta\varsigma_1)} \cdot \mathbf{D}_1(-\delta\alpha_1) \quad (12)$$

with $\delta\alpha_1 = (\delta\alpha_{1y}, \delta\alpha_{1z})$ the combination of rotation and displacement defined by Eq.(1) and \mathbf{D}_1 the displacement operator

$$\mathbf{D}_1(-\delta\alpha_1) = \exp(-\delta\alpha_{1q} \mathbf{B}_q^\dagger + \delta\alpha_{1q}^* \mathbf{B}_q)$$

acting on the functions of the transverse coordinates. The operators \mathbf{B}_y and \mathbf{B}_z act on the mode functions u_λ as typical annihilation operators, $\mathbf{B}u_n = \sqrt{n}u_{n-1}$, and this is the reason why \mathbf{D} has been called a displacement operator.

Next, the propagation from the input mirror to the opposite one is described by

$$e^{ik^\ell L} \left(\hat{D}_t \mathbf{\Phi} \right)^{\frac{1}{2}} \quad (13)$$

with $\hat{D}_t = e^{-\tau \frac{d}{dt}}$ the delay operator by the cavity round-trip time τ . Next combining (12) with (13) a round trip is represented by

$$R e^{-i\psi - i\delta\psi_{1,cav}} \left(\hat{D}_t \mathbf{\Phi} \right)^{\frac{1}{2}} \cdot e^{-i\delta\varsigma_2} \cdot \mathbf{D}_2(-\delta\alpha_2) \left(\hat{D}_t \mathbf{\Phi} \right)^{\frac{1}{2}} \cdot e^{-i\delta\varsigma_1} \cdot \mathbf{D}_1(-\delta\alpha_1)$$

where ψ is the detuning phase ($\psi > 0$ for a cavity shorter than the closest resonance length), $R = r_1 r_2 = e^{-\mathcal{F}/\pi}$ with \mathcal{F} the cavity finesse, and $\delta\psi_{1,cav}$ the accumulated phase shift, positive for decreasing cavity length,

$$\delta\psi_{1,cav}(t) = \delta\psi_1(t - \tau) + \delta\psi_2\left(t - \frac{\tau}{2}\right)$$

with $\delta\psi_J = -(-1)^J 2k^\ell \delta x_J$. Next, in view of the small-

ness of $\delta\psi_{1,cav}$, $\delta\alpha_J$ and $\delta\varsigma_J$ $\mathbf{D}_{1,2}$ and $e^{-i\delta\psi_{1,cav}}$ can be linearized thus obtaining for the round-trip transformation

$$e^{-i\psi} R \mathbf{\Phi} \left(\hat{D}_t - i\mathfrak{X} \cdot \delta\alpha_{J,cav} - i\delta\varsigma_{J,cav} \right). \quad (14)$$

Here $\mathfrak{X} \cdot \delta\alpha_{J,cav}$ indicates the sum $\mathfrak{X}_i (\delta\alpha_{J,cav})_i$ and two

vectors

$$\mathfrak{X} = (1, \mathbf{X}_y, \mathbf{X}_z, \mathbf{Y}_y, \mathbf{Y}_z) \quad (15)$$

$$\delta\alpha_{J,cav} = (\delta\psi_{J,cav}, \delta\alpha''_{Jy,cav}, \delta\alpha''_{Jz,cav}, \delta\alpha'_{Jy,cav}, \delta\alpha'_{Jz,cav})$$

collect the phase quadratures $\mathbf{X}_q = \mathbf{B}_q + \mathbf{B}_q^\dagger$, $\mathbf{Y}_q = i(\mathbf{B}_q - \mathbf{B}_q^\dagger)$ and the combinations

$$\delta\alpha_{1q,cav}(t) = \delta\alpha_{1q}(t - \tau) + e^{i\phi\sigma} \delta\alpha_{2q}\left(t - \frac{\tau}{2}\right)$$

(α' and α'' are the real and imaginary part of α respectively).

Analogously for $\delta\zeta_{J,cav}$

$$\delta\zeta_{1,cav}(t) = \zeta_{Js} \delta\zeta_{Js}(t - \tau) + \Phi^{-\frac{1}{2}} \cdot \zeta_{2s'} \cdot \Phi^{\frac{1}{2}} \delta\zeta_{2s'}\left(t - \frac{\tau}{2}\right)$$

The amplitude $a_{\lambda_y \lambda_z}^{(\sigma)}(t)$ of the $\lambda_y \lambda_z$ -th mode is propagated back and forth the cavity. The fraction t_1 is injected into the Fabry Perot through mirror 1 at time t , propagates toward and is reflected by mirror 2 at $t + \frac{\tau}{2}$ and again by 1 at t . Hence, summing over the sequence of round-trips, the field \mathbf{a}_J incident on the J -th mirror reads

$$\mathbf{a}_J = \mathcal{E}(1 + \mu^\ell) \hat{\mathbf{G}}_J \cdot \mathbf{v}_J F + \delta\hat{\mathbf{a}}^{SN} \quad (16)$$

with $\mathcal{E} = t_1 E$ and

$$\hat{\mathbf{G}}_J = \frac{1}{1 - Re^{-i\psi} \Phi \cdot \left(\hat{D}_t - i\mathfrak{X} \cdot \delta\alpha_{J,cav} - i\delta\zeta_{J,cav} \right)}$$

For very small $\delta\alpha_{J,cav}$ and $\delta\zeta_{J,cav}$ first-order perturbation theory can be used. On the other hand assuming for u_λ either Hermite or Laguerre-Gauss modes the various terms of the perturbation $\mathfrak{X} \cdot \delta\alpha_{J,cav} + \delta\zeta_{J,cav}$ do not couple the respective degenerate modes. Hence, the Green operator $\hat{\mathbf{G}}_J$ can be expressed as

$$\hat{\mathbf{G}}_J \simeq \hat{\mathbf{G}} - i\mathfrak{G} \cdot \delta\alpha_{J,cav} - i\delta\hat{\mathbf{G}}^{DEF} \quad (17)$$

where the first term on the right is a static propagator, the second the contribution of the linearized motion of the mirrors and the third one describes the mirror deformations,

$$\begin{aligned} \hat{\mathbf{G}} &= \left(1 - Re^{-i\psi} \hat{D}_t \Phi\right)^{-1} \\ \mathfrak{G} &= e^{-i\psi} R \hat{\mathbf{G}} \cdot \Phi \cdot \mathfrak{X} \cdot \hat{\mathbf{G}} \\ \delta\hat{\mathbf{G}}^{DEF} &= e^{-i\psi} R \hat{\mathbf{G}} \cdot \Phi \cdot \delta\zeta_{J,cav} \cdot \hat{\mathbf{G}} \end{aligned} \quad (18)$$

Next, the contributions of the shot noises entering the cavity through mirror J has been split as $\delta\hat{\mathbf{a}}^{SN} = \delta\hat{\mathbf{a}}_1^{SN} + t_2 t_1^{-1} \delta\hat{\mathbf{a}}_2^{SN}$, so that the same approximation of Eq. (18) applies and

$$\mathbf{a}_J = \mathbf{a}_{0,J} + \delta\mathbf{a}_J + \delta\hat{\mathbf{a}}^{SN} \quad (19)$$

Here $\delta\mathbf{a}_J$ is fluctuating with the cavity geometry and laser intensity, while $\mathbf{a}_{0,J}$ does not depend on it and on shot noise,

$$\begin{aligned} \mathbf{a}_{0,J} &\approx \mathcal{E} \hat{\mathbf{G}} \cdot \mathbf{v}_J F \\ \delta\mathbf{a}_J &\approx \mathcal{E} \left(\mu^\ell \hat{\mathbf{G}} - i\mathfrak{G} \cdot \delta\alpha_{J,cav} - i\delta\hat{\mathbf{G}}^{DEF} \right) \cdot \mathbf{v}_J F \\ \delta\hat{\mathbf{a}}^{SN} &= t_1 \hat{\mathbf{G}} \cdot \left(\delta\hat{\mathbf{a}}_1^{SN} + \frac{t_2}{t_1} \delta\hat{\mathbf{a}}_2^{SN} \right). \end{aligned} \quad (20)$$

Further, the relation $\hat{D}_t e^{-ip\Lambda t} = e^{-ip\Lambda t} e^{ip\Lambda\tau} \hat{D}_t$ implies $\hat{\mathbf{G}} e^{-ip\Lambda t} = e^{-ip\Lambda t} \hat{\mathbf{G}}_p$ with the suffix p indicating that R has been replaced by $R_p = e^{ip\Lambda\tau} R$. Then, the factor $e^{-ip\Lambda t}$ contained in the function F (see Eq. 6) can be displaced from the right to the left side of the above expressions by adding the suffix p to the various Green's functions. Hence

$$\mathbf{a}_J = e^{-ip\Lambda t} (\mathbf{a}_{0,Jp} + \delta\hat{\mathbf{a}}_{Jp}) + \delta\hat{\mathbf{a}}^{SN}$$

where

$$\begin{aligned} \mathbf{a}_{0,Jp} &= \mathcal{E} J_p \mathbf{G}_p \cdot \mathbf{v}_J \\ \delta\mathbf{a}_{Jp} &= e^{-ip\Lambda t} \mathcal{E} J_p \left(\mu^\ell \mathbf{G}_p - i\mathfrak{G}_p \cdot \delta\alpha_{J,cav} - i\delta\hat{\mathbf{G}}_p^{DEF} \right) \cdot \mathbf{v}_J \end{aligned} \quad (21)$$

Analogously for the output field [16]

$$\begin{aligned} \mathbf{a}_{0,Jp}^{OUT} &= t_1 \mathcal{E} J_p \mathbf{G}_p^{OUT} \cdot \mathbf{v}_1 \\ \delta\mathbf{a}_{Jp}^{OUT} &= t_1 \mathcal{E} J_p \left(\mathbf{G}_p^{OUT} \mu^\ell - i\mathfrak{G}_p \cdot \delta\alpha_{1,cav} - i\delta\hat{\mathbf{G}}_p^{DEF} \right) \cdot \mathbf{v}_1 \\ \delta\hat{\mathbf{a}}^{OUT SN} &= t_1^2 \left(\hat{\mathbf{G}}^{OUT} \cdot \delta\hat{\mathbf{a}}_1^{SN} + \frac{t_2}{t_1} \hat{\mathbf{G}} \cdot \delta\hat{\mathbf{a}}_2^{SN} \right) \end{aligned} \quad (22)$$

where $\hat{\mathbf{G}}^{OUT} = \hat{\mathbf{G}} - r_1/t_1^2$.

III. RADIATION PRESSURE AND TORQUE

Bouncing back and forth the two mirrors the laser and shot noise fields exert a radiation pressure resulting in an axial force directed along the optic axis \hat{x} and a torque parallel to their surfaces, proportional to the total intensity $\mathbf{a}_J^\dagger \cdot \mathbf{a}_J$ and moments $\mathbf{a}_J^\dagger \cdot \mathbf{X}_q \cdot \mathbf{a}_J$. They split into classical \mathcal{F}_{Jrp} , \mathcal{T}_{Jrp} and quantum \mathcal{F}_{rp}^{SN} , \mathcal{T}_{rp}^{SN} components respectively given by

$$\begin{aligned} \mathcal{F}_{Jrp} &= (-1)^J \mathcal{E}^2 2\Re_J \hbar k^\ell (F_{0,J} + \delta F_J) \hat{x} \\ \mathcal{T}_{Jrp} &= (-1)^J \mathcal{E}^2 2\Re_J \hbar k^\ell \frac{W_J}{\sqrt{2}} (T_{0,Jq} + \delta T_{Jq}) \hat{q} \times \hat{x} \end{aligned} \quad (23)$$

and

$$\begin{aligned} \mathcal{F}_{Jrp}^{SN} &\equiv (-1)^J \mathcal{E} 2\Re_J \hbar k^\ell \hat{X}_{J\psi}^{SN} \hat{x} \\ \mathcal{T}_{Jrp}^{SN} &\equiv (-1)^J \mathcal{E} 2\Re_J \hbar k^\ell \frac{W_J}{\sqrt{2}} \hat{X}_{J\theta q}^{SN} \hat{q} \times \hat{x} \end{aligned} \quad (24)$$

where $\Re_J = |r_J|^2 + \frac{1}{2} A_J$ with A_J the J -th mirror power absorption.

$F_{0,J}$ and δF_J indicate the contributions of $\mathbf{a}_{0,J}^\dagger \cdot \mathbf{a}_{0,J}$ and $\mathbf{a}_{0,J}^\dagger \cdot \delta \mathbf{a}_J + H.c.$ and analogously for $T_{0,Jq}, \delta T_{Jq}$. $F_{0,J}, T_{0,Jq}$ split in turn into time constant terms $\bar{F}_0, \bar{T}_{0,Jq}$, balanced by the stabilization system of the apparatus, and small terms $\delta F_{0,J}, \delta T_{0,Jq}$ oscillating at multiples of Λ . Being Λ typically of the order of some MHz these contributions can be ignored.

For a stabilized resonator $\tilde{\mathbf{G}}_J$ is represented as in (17) so that δF_J and δT_{Jq} reduce in the frequency domain respectively to

$$\begin{aligned} \delta \tilde{F}_J &= \bar{F}_{0,J} \tilde{\mu}^\ell + \tilde{\mathfrak{F}}_J \cdot \delta \alpha_{J,cav} + \delta \tilde{F}_{J,cav}^{DEF} \\ \delta \tilde{T}_{Jq} &= \bar{T}_{0,Jq} \tilde{\mu}^\ell + \tilde{\mathfrak{T}}_{Jq} \cdot \delta \tilde{\alpha}_{J,cav} + \delta \tilde{T}_{Jq,cav}^{DEF} \end{aligned} \quad (25)$$

The three pieces of Eqs. (25) represent, in the given order, the contributions of the fluctuation of laser intensity, mirror displacements, rotations and surface deformations to the radiation pressure forces and torques.

Being the suspension characteristic frequencies generally smaller than the mirror modes resonances [24], the deformations are described by a single matrix (see Eq. (11)).

The vectors $\tilde{\mathfrak{F}}_J = (F_{J\psi}, F_{JXq}, F_{JYq})$ and $\tilde{\mathfrak{T}}_{Jq} = (T_{J\psi q}, T_{JqXq'}, T_{JqYq'})$ contain five proportionality constants between the forces (the torques) and the coordinates ($\delta \tilde{\alpha}_{J,cav}$) which parametrize the mirror's displacement, so they are stiffness coefficients. $\bar{F}_{0,J}, \tilde{\mathfrak{F}}_J, \delta \tilde{F}_{J,cav}^{DEF}$ and $\bar{T}_{0,Jq}, \tilde{\mathfrak{T}}_{Jq}, \delta \tilde{T}_{Jq,cav}^{DEF}$ depend on the steady-state amplitudes of the cavity modes, represented by the vector \mathbf{v}_J ,

$$\begin{aligned} \bar{O}_{0,J} &= \mathbf{v}_J^\dagger \cdot \bar{\mathbf{O}}_0 \cdot \mathbf{v}_J \\ \tilde{O}_J &= \mathbf{v}_J^\dagger \cdot \tilde{\mathbf{O}} \cdot \mathbf{v}_J \end{aligned} \quad (26)$$

with $\bar{O}_{0,J} = \bar{F}_{0,J}, \bar{T}_{0,Jq}$ and $\tilde{O} = \tilde{\mathfrak{F}}_J, \delta \tilde{F}_{J,cav}^{DEF}, \tilde{\mathfrak{T}}_{Jq}$ and $\delta \tilde{T}_{Jq,cav}^{DEF}$. Matrices $\bar{\mathbf{F}}_0, \delta \tilde{\mathbf{F}}_{J,cav}^{DEF}$ and $\bar{\mathbf{T}}_{0,q}, \delta \tilde{\mathbf{T}}_{Jq,cav}^{DEF}$ are reported in Appendix A (Eqs. (A1,A4)) while $\tilde{\mathfrak{F}}, \tilde{\mathfrak{T}}_q$ are collections of five matrices (Eq. (A2)). They depend on Green's matrices (Eqs. (A3,A5)), and through them on frequency and detuning, closeness of cavity modes with respect to linewidth and phase modulation depth. The frequency dependence is due to the factor $e^{i\varpi\tau}$ appearing in different fashions in $\tilde{\mathbf{G}}_p, \tilde{\mathbf{G}}_p^{OUT}, \tilde{\mathbf{G}}_p$.

Eventually, the shot-noise contributions (Eq. (24)) are expressed by

$$\hat{\mathbf{X}}_{Ji}^{SN} = t_1^{-1} J_p \mathbf{v}_J^\dagger \cdot \mathbf{G}_p^\dagger \cdot \mathbf{X}_i \cdot \delta \hat{\mathbf{a}}^{SN} e^{ip\Lambda t} + H.c.$$

with $i \in (\psi, \theta_y, \theta_z)$ and take in the frequency domain the form

$$\tilde{\mathbf{X}}_{Ji}^{SN} = t_1^{-1} 2J_p \Re \left\{ \mathbf{v}_J^\dagger \cdot \mathbf{G}_p^\dagger \cdot \mathbf{X}_i \cdot \delta \tilde{\mathbf{a}}_p^{SN} \right\} \quad (27)$$

Finally, on the J 's mirror mode act the forces,

$$\begin{aligned} \mathcal{F}_{Jsrp}^{DEF} &= (-1)^J \mathcal{E}^2 2\Re_J \hbar k^\ell \\ &\quad (F_{0,J}^{DEF} + \delta F_{J,cav}^{DEF}) \hat{x} \\ \mathcal{F}_{Jsrp}^{DEF SN} &\equiv (-1)^J \mathcal{E} 2\Re_J \hbar k^\ell \hat{X}_{J_s}^{DEF SN} \hat{x} \end{aligned} \quad (28)$$

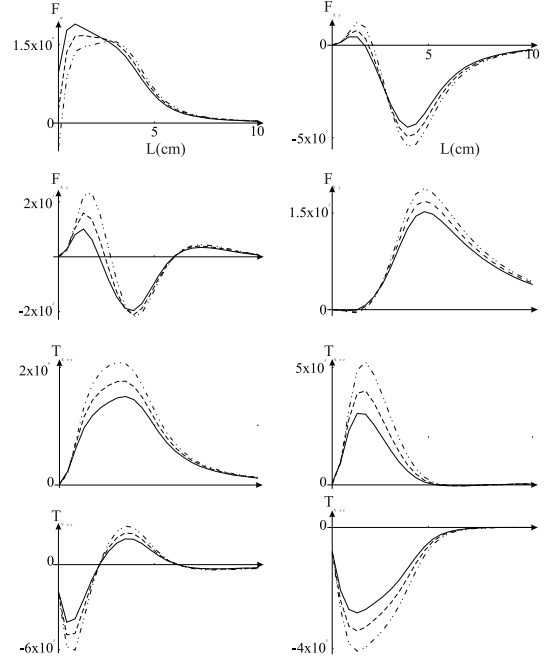


FIG. 2: Axial $F_\psi, F_{1Xy}, F_{1Xz}, F_{1Yy}$ and angular $T_{1zXz}, T_{1zYy}, T_{1zYz}$ stiffness coefficients vs. length L of a symmetric cavity for angular misalignments $\theta_y = .01, \theta_z = .1$ mrad and detunings $\psi = .1, .2, .3 \pi/F$. The round-trip phase factor $e^{i\varpi\tau}$ has been ignored.

where

$$\delta \tilde{F}_{J_s,cav}^{DEF} = e^{i\varpi\tau} \tilde{F}_{J_s J_s'}^{DEF} \delta \tilde{\zeta}_{J_s'} + e^{i\varpi\tau/2} \tilde{F}_{J_s J_s'}^{DEF} \delta \tilde{\zeta}_{J_s'}.$$

Here

$$\tilde{F}_{J_s J_s'}^{DEF} = \mathbf{v}_J^\dagger \cdot \tilde{\mathbf{F}}_{J_s J_s'}^{DEF} \cdot \mathbf{v}_J \quad (29)$$

is the force acting on the J_s -mode due to the deformations of the mirror surfaces. In this case the force does not factorize as for the suspension modes. $\tilde{\mathbf{F}}_{J_s J_s'}^{DEF}$ (Eq. (A6)) represent the effects of the vibrations of the modes J_s' on the J_s one.

Next, the shot-noise force is given by

$$\tilde{X}_{J_s}^{DEF SN} = t_1^{-1} 2J_p \Re \left\{ \mathbf{v}_J^\dagger \cdot \mathbf{G}_p^\dagger \cdot \zeta_{J_s} \cdot \delta \tilde{\mathbf{a}}_p^{SN} \right\} \quad (30)$$

In Fig. 2 the optically induced stiffness coefficients have been plotted for a set of detunings and angular misalignments, in an almost concentric cavity having a finesse $\mathcal{F} = 500$ and output spot sizes of $2 \times 10^{-3} m$. Being close to the concentric configuration also the stiffness coefficients $F_{X/Yq}, T_{zXy}, T_{yYz}$ become comparable with $F_\psi, T_{JqX/Yq}$ for cavity axis misaligned by $\theta_y = 10^{-2} rad, \theta_z = 10^{-1} rad$. The signs of the stiffness coefficients may have important consequences on the mechanical stability, as discussed by several authors for plane-parallel and concave mirrors [10, 18].

A. Small misalignment and mismatch

In the limit of small misalignment and mismatch the vector \mathbf{v}_1 (Eq. (4)) reduces to $\simeq \mathbf{1} + \delta\mathbf{v} = \{1, (\delta v_y, \delta v_z), 0, \dots, 0\}$ with

$$\delta\mathbf{v}_q = -\frac{\sqrt{2}}{w_1} \frac{Q^* Q_q}{Q^* - Q_q} \left(\theta_q - \frac{\varepsilon_q}{R_1} \right)$$

For mirror 2 \mathbf{v}_q is multiplied by $e^{-i\phi_G}$. Splitting forces and torques in 0-th and 1-st order terms in these misalignment parameters $\delta\tilde{F}_J$ and $\delta\tilde{T}_{Jq}$ of Eqs. (25) take the simpler forms,

$$\begin{aligned} \delta\tilde{F}_J &= \delta\tilde{F}_J^{(0)} + \delta\tilde{F}_J^{(1)} \\ \delta\tilde{T}_{Jq} &= \delta\tilde{T}_{Jq}^{(0)} + \delta\tilde{T}_{Jq}^{(1)} \end{aligned} \quad (31)$$

where

$$\begin{aligned} \delta\tilde{F}_J^{(0)} &= \tilde{F}_{0,J} \tilde{\mu}^\ell + \tilde{F}_\psi \delta\tilde{\psi}_{J,cav} + \delta\tilde{F}_{J,cav}^{DEF} \\ \delta\tilde{F}_J^{(1)} &= \delta\tilde{F}_{JXq} \delta\tilde{\alpha}''_{Jq,cav} + \delta\tilde{F}_{JYq} \delta\tilde{\alpha}'_{Jq,cav} \\ \delta\tilde{T}_{Jq}^{(0)} &= \tilde{T}_X \delta\tilde{\alpha}''_{Jq,cav} + \tilde{T}_Y \delta\tilde{\alpha}'_{Jq,cav} \\ \delta\tilde{T}_{Jq}^{(1)} &= \delta\tilde{T}_{Jq} \delta\tilde{\psi}_{J,cav} \end{aligned}$$

with

$$\begin{aligned} \delta\tilde{F}_{JX/Yq} &= 2 \operatorname{Re} \left\{ \tilde{F}_{X/Y} v_{Jq} \right\} \\ \delta\tilde{T}_{Jq} &= 2 \operatorname{Re} \left\{ \tilde{T}_\psi^{(1)} v_{Jq} \right\} \end{aligned}$$

$\tilde{F}_{X/Y}, \tilde{T}_\psi$ being defined in Appendix C. Accordingly, in the ideal setting of the cavity the forces and torques are respectively proportional to longitudinal $\delta\tilde{\psi}_{J,cav}$ and transverse $\delta\tilde{\alpha}''_{Jq,cav}$ fluctuations through the stiffness coefficients $\tilde{F}_\psi, \tilde{T}_{X/Y}$. A slight deviation from it introduces forces and torques with a reverse dependence on fluctuations, say $\delta\tilde{F}_J^{(1)}, \delta\tilde{T}_{Jq}^{(1)}$ depend respectively on $\delta\tilde{\alpha}_{Jq,cav}$ and $\delta\tilde{\psi}_{J,cav}$.

IV. ERROR SIGNALS

The errors used for controlling the cavity are provided by Drever-Pound (DP) and quadrant detector signals (QD). In the DP detection technique the photodetector current $I(t)$, obtained from the light transmitted and reflected by the input mirror, is mixed with a local oscillator $\sim \sin(k\Lambda t + \varphi)$ with positive odd integer k and low-pass filtered by an averaging procedure

$$s^{DP}(t) = \int_{-\infty}^t K^{DP}(t-t') \sin(k\Lambda t' + \varphi) I(t') dt' \quad (32)$$

with the filter response $K^{DP}(t-t')$ extended to a suitable interval much longer than $(k\Lambda)^{-1}$, and short compared to the time scale of the phase-quadrature fluctuations. Tuning φ around 0 s^{DP} can be maximized for a misaligned cavity.

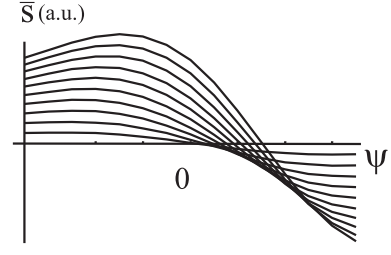


FIG. 3: Drever-Pound static characteristics \bar{s} vs. ψ for cavity lengths $1 \div 10$ cm and $\varphi = 0$. The plots correspond to modulation frequency $\Lambda = 2c\lambda^\ell / (\pi w^2)$, depth $M = 0.1$, and jaw angle $\delta\theta_z = 0.01$.

Putting $\delta\tilde{\mathbf{a}}_p^{SN} = \delta\tilde{\mathbf{a}}^{SN} (\varpi + p\Lambda)$, s^{DP} is represented in the frequency domain by

$$\begin{aligned} \tilde{s}^{DP} / \tilde{K}^{DP} &= \mathcal{E}^2 \left(\tilde{s}^{DP} \tilde{\mu}^\ell + \tilde{\mathbf{s}}^{DP} \cdot \delta\alpha_{cav} + \delta\tilde{s}^{DP DEF} \right) \\ &\quad + \mathcal{E} \tilde{X}^{DP SN} \end{aligned} \quad (33)$$

where

$$\begin{aligned} \tilde{s}^{DP} &= \mathbf{v}_1^\dagger \cdot \mathbf{I}^{DP} \cdot \mathbf{v}_1 \\ \tilde{\mathbf{s}}^{DP} &= \mathbf{v}_1^\dagger \cdot (\mathcal{J}_+^{DP} - \mathcal{J}_-^{DP}) \cdot \mathbf{v}_1 \\ \delta\tilde{s}^{DP DEF} &= \mathbf{v}_1^\dagger \cdot \left(\delta\tilde{\mathbf{I}}_+^{DP DEF} - \delta\tilde{\mathbf{I}}_-^{DP DEF} \right) \cdot \mathbf{v}_1 \\ \tilde{X}^{DP SN} &= \tilde{X}_+^{DP SN} - \tilde{X}_-^{DP SN} \end{aligned}$$

with $\mathbf{I}^{DP}, \delta\tilde{\mathbf{I}}_\pm^{DP DEF}, \tilde{\mathcal{J}}_\pm^{DP}, \tilde{X}_\pm^{DP SN}$ defined in Appendix B.

In Figure 3 the static characteristic \bar{s}^{DP} versus ψ has been plotted for a set of cavity lengths and modulations.

Figure 4 contains plots of the coefficients s_ψ and s_{Xy} vs. cavity length for $\varphi = 0$, $\theta_z = .1$ mrad and 7 detunings. They show that as a consequence of the misalignment s_{Xy} becomes comparable to s_ψ , so that the D-P error signal contains contributions of the torsional fluctuations around the vertical axis.

At low frequency $\delta\tilde{s}^{DP DEF}$ becomes proportional to the thermal noises $\delta\zeta^{LTH}$.

The quadrant detector used for stabilizing the angular oscillations provides two error signals $s_q^{QD}(t)$ ($q = y, z$), proportional to expressions similar to (32) with the current I replaced by $I_q = \beta^\dagger \cdot \mathbf{Q}_q \cdot \beta$ with

$$\beta = e^{-ip\Lambda t} \mathbf{a}_p^{OUT} + \delta\tilde{\mathbf{a}}^{OUT SN},$$

the matrix \mathbf{Q}_q representing the function $sgn(\bar{q})$. Then, \tilde{s}_q^{QD} is given by an expression similar to (33) with $\mathbf{G}_p^{OUT\dagger}$ replaced by $\mathbf{G}_p^{OUT\dagger} \cdot \mathbf{Q}_q$.

A. Small misalignment and mismatch

In the limit of small misalignment and mismatch the signal can be split into zeroth- and first-order contributions

$$\tilde{s}^{DP} = \tilde{s}^{(0)} + \delta\tilde{s}^{(1)}$$

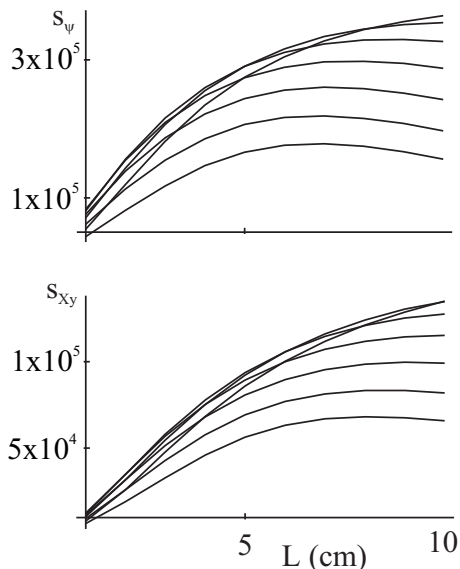


FIG. 4: Coefficients s_ψ and s_{xy} vs. cavity length for $\varphi = 0$, $\theta_z = .1$ mrad and 7 detunings ranging in the interval $-.3\frac{\pi}{\mathcal{F}} \leq \psi \leq .3\frac{\pi}{\mathcal{F}}$.

given respectively by (Eqs. (C4))

$$\begin{aligned} \tilde{s}^{(0)}/\tilde{K}^{DP} &= \mathcal{E}^2 \left(\tilde{s}_\psi \tilde{\mu}^\ell + \tilde{s}_\psi \delta \tilde{\psi}_{1,cav} + \delta \tilde{s}^{(0) DEF} \right) \\ &\quad + \mathcal{E} \tilde{X}^{SN(0)} \\ \delta \tilde{s}^{(1)}/\tilde{K}^{DP} &= \mathcal{E}^2 \left(\delta \tilde{s}_{Xq} \delta \tilde{\alpha}''_{1q,cav} + \delta \tilde{s}_{Yq} \delta \tilde{\alpha}'_{1q,cav} \right. \\ &\quad \left. + \delta \tilde{s}^{(1) DEF} \right) + \mathcal{E} \delta \tilde{X}^{SN(1)} \end{aligned} \quad (34)$$

with $\delta \tilde{s}_{X/Yq} = 2\text{Re} \{ \tilde{s}_{X/Y} v_{1q} \}$ and $\tilde{s}_{X/Y}$ defined in Appendix C.

For a perfectly aligned and matched cavity the D-P signal is sensitive to the axial fluctuations $\delta \tilde{\psi}_{1,cav}$, mirror deformation term $\delta \tilde{s}^{(0) DEF}$ and shot noise $\tilde{X}^{SN(0)}$. In particular, a contribution $\delta \tilde{\psi}_{1,cav}$ depending on the mirror thermal noise $\delta \tilde{\zeta}_{1,2}^L$ is added to the length fluctuation. A deviation from alignment introduces in the error signal contributions proportional to the transverse fluctuations.

V. 3D MODEL

The deviations of each mirror from the reference position is described by the displacements $\delta x, \delta \varepsilon_y$ and $\delta \varepsilon_z$ of its vertex and the angular parameters $\delta \theta_z = -\delta \Omega_y$ and $\delta \theta_y = \delta \Omega_z$. As said $\delta \Omega_q$ describes a right-handed rotations around the axis "q", so that $\delta \theta_z$ is a left-handed tilt and $\delta \theta_y$ a right-handed torsion. These quantities fluctuate as a consequence of suspension thermal fluctuations and mirror surface deformations. The radiation pressure fluctuations are transferred to the mirrors proportionally with the laser intensity. The cavity reacts by changes of geometry which in turn changes the stored field and closes the loop of the cavity-field system.

From a purely-mechanical point of view if the design is good (that is, symmetric enough) the suspension masses are aligned along the vertical axis z, perpendicular to the cavity axis x. In these conditions the torsion $\delta \theta_y$ and vertical $\delta \varepsilon_z$ degrees of freedom are uncoupled. A coupling between longitudinal motion δx and tilt $\delta \theta_z$ is generally speaking unavoidable. This is true also for the transverse displacement $\delta \varepsilon_y$ which is coupled with the rotation around the optical axis. It goes without saying that in a real situation it is very difficult to avoid more general cross couplings.

Radiation pressure can increase or reduce existing couplings, and it can also produce new ones. While $\delta \varepsilon_q$ is insensitive to radiation pressure, $\delta \theta_q$ responds to the radiation torque. For this reason when asymmetric optical modes are excited the rotations $\delta \theta_q$ modify the radiation pressure, and ultimately couple δx and tilting, but also δx and torsion.

Before proceeding further it is worth replacing the displacements $\delta \varepsilon_{Jq}$ by $\delta \psi_{Jq} = 2k^\ell \delta \varepsilon_{Jq}$, the angles $\delta \theta_{Jq}$ by $\delta \vartheta_{Jq} = \sqrt{2}k^\ell w_J \delta \theta_{Jq}$ and introducing a new five component vector $\delta \psi_J = (\delta \psi_J, \delta \psi_{Jq}, \delta \vartheta_{Jq})$ which forms with the cavity mode amplitudes a system of correlated stochastic processes. It is usually a very good approximation to model the suspension as a set of damped, independent oscillators coupled to an heat bath. Each oscillator $J\lambda \hat{j}$, labelled by λ , specifying the prevalent character of the mode (tilting, torsion, displacements, violin modes), and the mode index \hat{j} , can be parameterized with its effective mass $M_{J\lambda \hat{j}}$, pulsation $\varpi_{J\lambda \hat{j}}$ and damping coefficient $\gamma_{J\lambda \hat{j}}$. For rotations $M_{J\lambda \hat{j}}$ is replaced by the moment of inertia. These parameters are related to the masses and stiffness constants of the system. The coordinates of the mirror can be written as linear combinations of the oscillator's coordinates q_n , and this means that each normal mode gives in principle a contribution to the mirror's motion. By interacting with thermal baths these modes undergo Brownian motions by influencing the electromagnetic field, eventually coupling mechanical and radiation pressure fluctuations.

A. Suspension Langevin system

By linearizing the equation of motion of each mirror (J) the horizontal (x and y) and vertical (z) displacements $\delta \tilde{\psi}_J$, torsion $\delta \tilde{\vartheta}_{Jy}$, tilt $\delta \tilde{\vartheta}_{Jz}$ and rotation around the cavity axis $\delta \tilde{\vartheta}_{Jx}$ are expressed in terms of the amplitudes $\tilde{A}_{J\lambda \hat{j}}$ of the normal modes as

$$\delta \tilde{\psi}_{J\mu} = K_{J\mu \lambda \hat{j}} \tilde{A}_{J\lambda \hat{j}}$$

having indicated by $J\mu$ a generic degree of freedom and by $K_{J\mu \lambda \hat{j}}$ the coupling coefficient with the mode $J\lambda \hat{j}$ [27].

If the mirror vertex coincides with the center of mass of the suspension payload, and the centers of the suspended masses are aligned along the vertical z -axis, the suspension can be easily modeled by considering only the

couplings $\delta\psi_J - \delta\tilde{\vartheta}_{Jz}$ and $\delta\psi_{Jy} - \delta\tilde{\vartheta}_{Jx}$, and assuming the vertical oscillations independent of the other degrees of freedom. Being the amplitudes of the cavity modes independent of the rotations $\delta\tilde{\vartheta}_{Jx}$, the suspended cavity is described by the collection $\delta\psi_J$ of five fluctuating quantities, depending linearly on radiation pressure-torques, thermal noise, D-P and quadrant detector error signals,

$$\begin{aligned}
\delta\tilde{\psi}_J &= \tilde{\chi}_{J\psi} 8\Re_J \left(\mathcal{E}^2 \delta\tilde{F}_J + \mathcal{E} \tilde{X}_{J\theta z}^{SN} \right) \\
&\quad + \tilde{\chi}_{J\psi\theta z} \delta\Re_J \left(\mathcal{E}^2 \delta\tilde{T}_{Jz} + \mathcal{E} \tilde{X}_{J\theta z}^{SN} \right) \\
&\quad + \tilde{\chi}_{J\psi}^{TH} + \delta_{J1} H^{DP} \tilde{s}^{DP} \\
\delta\tilde{\psi}_{Jy/z} &= \tilde{\chi}_{Jy/z}^{TH} \\
\delta\tilde{\vartheta}_{Jz} &= \tilde{\chi}_{J\theta z\psi} 8\Re_J \left(\mathcal{E}^2 \delta\tilde{F}_J + \mathcal{E} \tilde{X}_{J\theta z}^{SN} \right) \\
&\quad + \tilde{\chi}_{J\theta z} \delta\Re_J \left(\mathcal{E}^2 \delta\tilde{T}_{Jz} + \mathcal{E} \tilde{X}_{J\theta z}^{SN} \right) \\
&\quad + \tilde{\chi}_{J\theta z}^{TH} + \delta_{J1} H_z^{QD} \tilde{s}_z^{QD} \\
\delta\tilde{\vartheta}_{Jy} &= \tilde{\chi}_{J\theta y\psi} 8\Re_J \left(\mathcal{E}^2 \delta\tilde{T}_{Jy} + \mathcal{E} \tilde{X}_{J\theta y}^{SN} \right) \\
&\quad + \tilde{\chi}_{J\theta y}^{TH} + \delta_{J1} H_y^{QD} \tilde{s}_y^{QD} \tag{35}
\end{aligned}$$

In case the mirror vertex and/or the centers of the suspension wire clampings are displaced from the respective mass centers, the vertical fluctuations are coupled to the other ones.

The effect of the servo systems acting on the longitudinal and angular mirror displacements have been included by indicating by \tilde{H}^{DP} and \tilde{H}_q^{QD} the respective transfer functions.

For the mirror vibrations a Langevin equation for each mode must be considered since their profiles are different (Eq. (30)),

$$\delta\tilde{\zeta}_{Js} = 8\tilde{\chi}_{Js} \left(\mathcal{E}^2 \delta\tilde{F}_{Js,cav}^{DEF} + \mathcal{E} \tilde{X}_{Js}^{DEF SN} \right) + \tilde{\chi}_{Js}^{DEF TH} \tag{36}$$

Expressing $\delta\tilde{F}_J$, $\delta\tilde{T}_{Jq}$ in terms of displacements and rotations by introducing the stiffness coefficients, and doing the same for the error signals \tilde{s}^{DP} , \tilde{s}_q^{QD} the above system can be reduced to an equivalent one relating the fluctuating displacement + rotations to the thermal noise and shot noise sources.

The axial displacement $\delta\tilde{\psi}_J$ and tilting $\delta\tilde{\vartheta}_{Jz}$ respond to the axial force $\mathcal{E}^2 \delta\tilde{F}_J + \mathcal{E} \tilde{X}_{J\theta z}^{SN}$ and torque $\left(\mathcal{E}^2 \delta\tilde{T}_{Jz} + \mathcal{E} \tilde{X}_{J\theta z}^{SN} \right) \hat{y}$ generated by the laser beam and the shot noise. By the way they include the contributions of the mirror thermal noise. On the other hand, $\delta\tilde{\vartheta}_{Jy}$ responds to the torque $\mathcal{E}^2 \delta\tilde{T}_{Jy} + \mathcal{E} \tilde{X}_{J\theta y}^{SN}$. The links between force-torques and $\delta\tilde{\psi}_J$ are represented by the susceptibilities $\tilde{\chi}_{J\mu\nu}$.

The terms proportional to \mathcal{E}^2 and \mathcal{E} describe the response of the system to radiation pressure. Their presence indicates that a motion of the mirrors produces not only a phase change but also an intensity change providing a spring action.

In writing Eq. (35) the interaction with the mirror noise was approximated with Eq. (11) while in Eq. (36) the effects of the suspension fluctuations were ignored. Loosely speaking the two systems refer respectively to the low and high frequency regions. In the former one the suspensions are mutually coupled by radiative forces represented while the mirror vibrations generate a global thermal noise hiding the single mode contributions. In the latter one the suspensions appear frozen and the mirror modes are mutually coupled by radiative forces represented by $\delta\tilde{F}_{Js,cav}^{DEF}$.

The solutions of the homogeneous system (35) represent, in absence of feedback forces, free mechanical oscillations of the suspended cavity, stable or unstable in accordance with the sign of the imaginary part of the oscillation frequency [20].

For a more detailed analysis (35) and (36) should be mirrored by the system relative to the quantities $\delta\tilde{\psi}_J^Y$, $\delta\tilde{\zeta}_{Js}^Y$ conjugate of $\delta\tilde{\psi}_J$, $\{\delta\zeta_{Js}\}$, which can be obtained from the above one by replacing $\tilde{\chi}_{J\psi/\theta q/s}$ by $\tilde{\chi}_{J\psi/\theta q/s}^Y$ (Eq. 40) and $\tilde{X}_{J\psi/\theta q}^{TH}$, $\tilde{X}_{Js}^{DEF TH}$ by $\tilde{Y}_{J\psi/\theta q}^{TH}$, $\tilde{Y}_{Js}^{DEF TH}$ (Eq. 41) in the random force expressions.

B. Susceptibilities

The susceptibility $\tilde{\chi}_{J\mu\nu}$ describes the action on the coordinate μ of the force/torque acting on ν ,

$$\tilde{\chi}_{J\mu\nu} = K_{J\mu\lambda\hat{j}} K_{J\nu\lambda\hat{j}} \tilde{\chi}_{J\lambda\hat{j}}$$

with $\tilde{\chi}_{J\lambda\hat{j}}$ the susceptibility of the mode $J\lambda\hat{j}$ of frequency $\varpi_{J\lambda\hat{j}}$ and damping coefficient $\gamma_{J\lambda\hat{j}}$

$$\tilde{\chi}_{J\lambda\hat{j}} = \frac{\varpi_{J\lambda\hat{j}} \eta_{J\lambda\hat{j}}^{LD 2}}{\varpi_{J\lambda\hat{j}}^2 - \varpi^2 - i\varpi \gamma_{J\lambda\hat{j}}} \tag{37}$$

and $K_{J\mu\lambda\hat{j}}$, $K_{J\nu\lambda\hat{j}}$ the coupling coefficients with μ and ν mirror coordinates, while the adimensional Lamb-Dicke factor

$$\eta_{J\lambda\hat{j}}^{LD} = k^\ell \sqrt{\frac{\hbar}{2M_{J\lambda\hat{j}} \varpi_{J\lambda\hat{j}}}} \tag{38}$$

depends on the mode mass $M_{J\lambda\hat{j}} = M_{Ji} K_{Ji\lambda\hat{j}}^2$ (the subfix i identifies the i -th mass of the suspension). For rotations $M_{J\lambda\hat{j}}$ is replaced by $I_{J\lambda\hat{j}}/w_{\hat{j}}^2$ with $I_{J\lambda\hat{j}}$ the moment of inertia. Some authors use the so-called optomechanical coupling constants $G_{J\lambda\hat{j}} = 2\sqrt{2}\eta_{J\lambda\hat{j}}^{LD}/\tau$ [21].

The mechanical susceptibility $\tilde{\chi}_{Js}$ is similar to (37) while the mass appearing in the Lamb-Dicke factor varies for the different modes, as reported in [24].

C. Thermal contributions

Assuming suspension masses at the same temperature T , each mode is characterized by a thermal source (see

Appendix D)

$$\tilde{X}_{J\lambda_j}^{TH} = \sqrt{\frac{4k_B T}{\hbar\varpi_{J\lambda_j}}} \tilde{\xi}_{J\lambda_j} - i \frac{\varpi + i\gamma_{J\lambda_j}}{\varpi_{J\lambda_j}} \sqrt{\frac{\hbar\varpi_{J\lambda_j}}{3k_B T}} \tilde{\eta}_{J\lambda_j} \quad (39)$$

with $\tilde{\eta}, \tilde{\xi}$ delta correlated random forces introduced by Diosi [12] in order to remove some inconsistencies of the classical Langevin equation.

A Y-version of (35) can be easily obtained for the Y-quadratures corresponding to the above ones by replacing $\tilde{\chi}_{J\mu\lambda_j}$ by

$$\tilde{\chi}_{J\lambda_j}^Y = i \frac{\varpi}{\varpi_{J\lambda_j}} \tilde{\chi}_{J\lambda_j} \quad (40)$$

and $\tilde{X}_{J\lambda_j}^{TH}$ by

$$\tilde{Y}_{J\lambda_j}^{TH} = \sqrt{\frac{4k_B T}{\hbar\varpi_{J\lambda_j}}} \tilde{\xi}_{J\lambda_j} - i \frac{\varpi_{J\lambda_j}}{\varpi} \sqrt{\frac{\hbar\varpi_{J\lambda_j}}{3k_B T}} \tilde{\eta}_{J\lambda_j} \quad (41)$$

The terms proportional to $\tilde{\eta}_{J\lambda_j}$ in Eqs. (39) and (41) can be generally neglected except when the temperature is rather low and the oscillation frequencies very high, a situation met only in some mirror modes.

$\tilde{\eta}_{J\lambda_j}$ disappears in the simple Brownian motion model while in Ref. [14] $\tilde{\eta}_{J\lambda_j}$ has been dropped and $\sqrt{\frac{4k_B T}{\hbar\varpi_{J\lambda_j}}} \tilde{\xi}_{J\lambda_j}$ replaced by a new delta correlated random noise source $\tilde{Q}_{J\lambda_j}$.

The thermal sources $\tilde{\mathcal{X}}_{J\mu}^{TH}$ are superpositions

$$\tilde{\mathcal{X}}_{J\mu}^{TH} = K_{J\mu\lambda_j} \tilde{\chi}_{J\lambda_j}^{TH} \tilde{X}_{J\lambda_j}^{TH}$$

of the $\tilde{X}_{J\lambda_j}^{TH}$ weighted by the thermal susceptibilities

$$\tilde{\chi}_{J\lambda_j}^{TH} = \kappa_{J\lambda_j} \tilde{\chi}_{J\lambda_j} \quad (42)$$

with $\kappa_{J\lambda_j} = 2\sqrt{\gamma_{J\lambda_j}}/\eta_{J\lambda_j}^{LD}$.

The terms of (35) contain contributions proportional to the fluctuating quantities $\delta\zeta_J^{L TH}$ [26]

$$\delta\zeta_J^{L TH} = \sqrt{\frac{4k_B T}{\hbar\varpi}} \sqrt{2\hbar k^l c_P \phi_J \zeta} \quad (43)$$

with ϕ the loss angle, ζ a delta correlated random force and c_P depending on the illumination profile

$$P(\vec{r}) = P_{\lambda_y, \lambda_z} e^{-\frac{r^2}{2w^2}} u_{\lambda_y, \lambda_z}(\vec{r}) \quad (44)$$

For $P(\vec{r})$ differing notably from the Gaussian one the deformed profile of the mirror $\delta u_{1,2}^{DEF}$ can be expressed, neglecting the finite size of the mirrors, by a suitable combination of derivatives of the deformation $\delta u_G^{DEF}(\vec{r})$ relative to a Gaussian distribution

$$\delta u^{DEF}(\vec{r}) = \sum_{\lambda_y, \lambda_z} P_{\lambda_y, \lambda_z} (-w)^{\lambda_y + \lambda_z} \frac{\partial^{\lambda_y}}{\partial y^{\lambda_y}} \frac{\partial^{\lambda_z}}{\partial z^{\lambda_z}} \delta u_G^{DEF}(\vec{r})$$

For a Gaussian illumination c_P takes the form

$$c_G = \frac{1 - \sigma^2}{\sqrt{2\pi} E w_J}$$

with w_J the spot-size and E, σ the Young's modulus and Poisson ratio respectively. For a generic illumination c_P can be expressed as $c_P = f_P c_G$ with

$$f_P = \sum_{\lambda\lambda'} (-1)^{\lambda'_y + \lambda'_z} \frac{P_{\lambda_y, \lambda_z} P_{\lambda'_y, \lambda'_z}}{P_{00}^2} f_{\lambda_y + \lambda'_y, \lambda_z + \lambda'_z} \quad (45)$$

$f_{\alpha\beta}$ being the $\alpha\beta$ coefficient of the expansion of $\delta u_G(\vec{r}) e^{-\frac{r^2}{2w^2}}$ in modes $u_{\lambda_y, \lambda_z}(\vec{r})$.

VI. THE SUSPENDED CAVITY AS A BIPARTITE SYSTEM

When the frequency is in proximity of two close resonances of the mirror 1 and 2 modes, the system behaves as a quantum mechanical bipartite system described by Gaussian continuous variables. These systems can form EPR states characterized by their covariance matrix σ which can be used for evaluating the entanglement of the state and its content of quantum information.

The difference between the e.m. fields used in quantum optics and the present mechanical system concerns the sources of the respective states. The e.m. fields are produced by the e.m. vacuum noise entering through the mirrors of a cavity containing a nonlinear crystal. In the present case thermal and shot noises act as sources. Accordingly, the covariance matrix σ can be split into thermal σ^{TH} and shot noise $(8\mathcal{E})^2 \sigma^{SN}$ contributions obtained by separating $\delta\zeta_J$ into $\delta\zeta_J = 8\mathcal{E} \delta\zeta_J^{SN} + \delta\zeta_J^{TH}$ satisfying the Langevin system (36)

$$\begin{bmatrix} \delta\zeta_1^{SN/TH} \\ \delta\zeta_2^{SN/TH} \end{bmatrix} = \frac{1}{D} \begin{bmatrix} \tilde{\mathcal{P}}_{22} & -\tilde{\mathcal{P}}_{12} \\ -\tilde{\mathcal{P}}_{21} & \tilde{\mathcal{P}}_{11} \end{bmatrix} \cdot \begin{bmatrix} \chi_1 \tilde{X}_1^{DEF SN/TH} \\ \chi_2 \tilde{X}_2^{DEF SN/TH} \end{bmatrix} \quad (46)$$

with $\tilde{\mathcal{P}}_{JJ'}$ factors representing the radiation pressure effects

$$\begin{aligned} \tilde{\mathcal{P}}_{JJ} &= 1 - 8e^{i\varpi\tau} \mathcal{E}^2 \Re_J \tilde{\chi}_J \tilde{F}_{JJ}^{DEF} \\ \tilde{\mathcal{P}}_{J\bar{J}} &= 8e^{i\varpi\tau/2} \mathcal{E}^2 \Re_J \tilde{\chi}_J \tilde{F}_{J\bar{J}}^{DEF} \end{aligned}$$

and their product $\tilde{D} = \tilde{\mathcal{P}}_{11} \tilde{\mathcal{P}}_{22} - \tilde{\mathcal{P}}_{12} \tilde{\mathcal{P}}_{21}$. An analogous system holds for $\delta\zeta_J^{SN}$ with $\tilde{\chi}_J$ replaced by $\tilde{\chi}_J^Y$.

The output field contains a component (Eqs. (18,22))

$$\delta \tilde{\mathbf{a}}^{OUT} \propto \left(e^{i\varpi\tau} \tilde{\mathbf{Z}}_1 \delta\zeta_1 + e^{i\varpi\tau/2} \tilde{\mathbf{Z}}_2 \delta\zeta_2 \right) \cdot \mathbf{v}_1$$

proportional to $\delta\zeta_{1,2}$ through the matrices $\tilde{\mathbf{Z}}_J = \mathbf{G} \cdot \tilde{\Phi} \cdot \zeta_J \cdot \tilde{\mathbf{G}}$ and a shot noise $\tilde{\mathbf{G}}^{OUT} \cdot \delta \tilde{\mathbf{a}}_1^{SN} + \frac{t_2}{t_1} \tilde{\mathbf{G}} \cdot \delta \tilde{\mathbf{a}}_2^{SN}$ term. Hence, depending $\delta\zeta_{1,2}^{SN}$ linearly on the quadratures $\tilde{X}_{1,2}^{DEF SN}$ the output exhibits some degree of

squeezing., a feature exploited by several groups in the context of gravitational antennas of the next generation [22]. The dependence of the efficiency of the ponderomotive squeezing on the mirror deformation profiles (matrices $\tilde{\mathbf{Z}}_J$) and residual misalignment/mismatch can be easily analyzed by means of Eqs. (46) and the correlations of Apps. E and F.

The complex dynamics of cavity field and ponderomotive effects may lead to the creation of quantum entangled states of the two mirror modes, as shown by Mancini et al. ([21] and references therein included). These authors have proposed a measure $\mathbb{E}(\varpi)$ of the entanglement degree (the smaller $\mathbb{E}(\varpi) < 1$ the larger the entanglement) based on a combination of the elements of the covariance matrix,

$$\mathbb{E}(\varpi) = \frac{|\delta\tilde{\zeta}_1 + \delta\tilde{\zeta}_2|^2 |\delta\tilde{\zeta}_1^Y - \delta\tilde{\zeta}_2^Y|^2}{\left|[\delta\tilde{\zeta}_1, \delta\tilde{\zeta}_1^Y]\right|^2} \quad (47)$$

Splitting the quadratures into shot noise and thermal contributions, taking into account the many modes of the cavity and the shapes of the mirror mechanical modes, and scaling the ratio terms by keeping constant $\mathbb{E}(\varpi)$, yield for the thermal and the shot noise contributions

$$\begin{aligned} |\delta\tilde{\zeta}_1^{TH} + \delta\tilde{\zeta}_2^{TH}|^2 &= |\chi_J^{TH}|^2 \tilde{C}_J^{TH X(+)} \quad (48) \\ -\frac{i}{2} \overline{[\delta\tilde{\zeta}_1^{TH}, \delta\tilde{\zeta}_1^{THY}]} &= \left(\frac{\varpi}{\varpi_J}\right)^2 |\alpha_J \chi_J^{TH}|^2 \\ |\delta\tilde{\zeta}_1^{SN} + \delta\tilde{\zeta}_2^{SN}|^2 &= \chi_J \chi_{J'}^* \tilde{C}_{JJ'}^{SN X(+)} \\ \overline{[\delta\tilde{\zeta}_1^{SN}, \delta\tilde{\zeta}_1^{SNY}]} &= \frac{\varpi(\varpi_J + \varpi_{J'})}{2\varpi_J \varpi_{J'}} \tilde{\chi}_J \tilde{\chi}_{J'}^* \alpha_J \alpha_{J'}^* \tilde{C}_{JJ'}^{SN Y} \end{aligned}$$

with χ_J^{TH} defined in (42), while $|\delta\tilde{\zeta}_1^{TH} - \delta\tilde{\zeta}_2^{TH}|^2$ and $|\delta\tilde{\zeta}_1^{SN} - \delta\tilde{\zeta}_2^{SN}|^2$ are similar to (48)–a and –c with χ_J , $\tilde{C}_J^{TH X(+)}$ and $\tilde{C}_{JJ'}^{SN X(+)}$ replaced respectively by χ_J^Y , $\tilde{C}_J^{TH Y(-)}$ and $\frac{\varpi^2}{\varpi_J \varpi_{J'}} \tilde{C}_{JJ'}^{SN X(-)}$. On the other hand,

$$(\alpha_1, \alpha_2) = \left(\tilde{\mathcal{P}}_{22}, \tilde{\mathcal{P}}_{12} \right) \left| \tilde{\mathcal{P}}_1^{(+)} \tilde{\mathcal{P}}_2^{(+)} \tilde{\mathcal{P}}_1^{(-)} \tilde{\mathcal{P}}_2^{(-)} \right|^{-1/2},$$

$$\tilde{\mathcal{P}}_J^{(\pm)} = \tilde{\mathcal{P}}_{JJ} \pm \tilde{\mathcal{P}}_{J\bar{J}}$$

$$\begin{aligned} \tilde{C}_J^{TH X/Y(\pm)} &= \frac{\text{Re} \left\{ \tilde{C}_J^{XX/YY TH} \right\}}{2 \left| \tilde{\mathcal{P}}_J^{(\pm)} \right|^2} \\ \tilde{C}_{JJ'}^{SN X(\pm)} &= \frac{\text{Re} \left\{ \tilde{C}_{JJ'}^{SN} \right\}}{2 \left| \tilde{\mathcal{P}}_J^{(\pm)*} \tilde{\mathcal{P}}_{J'}^{(\pm)} \right|} \\ \tilde{C}_{JJ'}^{SN Y} &= \frac{\text{Im} \left\{ \tilde{C}_{JJ'}^{SN} \right\}}{2 \sqrt{\left| \tilde{\mathcal{P}}_1^{(+)} \tilde{\mathcal{P}}_2^{(+)} \tilde{\mathcal{P}}_1^{(-)} \tilde{\mathcal{P}}_2^{(-)} \right|}} \end{aligned}$$

with $\tilde{C}_{J\bar{s}J's'}^{SN}$ given by Eq. (F2). In App. E thermal noise correlations for the Lindblad–Diosi and the Giovanetti–Vitali MEs are explicitly given.

VII. CONCLUSIONS

A suspended cavity illuminated by a laser beam has been described as the mechanical response $\delta\psi_J$ of each mirror of a linear system to radiative, thermal and shot noise forces. These perturbations have been linked to the mechanical responses by means of susceptibility coefficients. The model includes the mirror vibrations described by a set of mode amplitudes $\delta\zeta$, together with their shapes ς .

The radiative pressure forces and torques have been linearized with respect to $\delta\psi_J$ and $\delta\zeta$, by obtaining sets of stiffness coefficients for the suspension (\mathfrak{F} and \mathfrak{T}) and for the mirror modes ($F_{J\bar{s}J's'}^{DEF}$). Accordingly the radiative forces have been expressed as products of susceptibility coefficients, laser intensity transmitted to the cavity (\mathcal{E}^2), stiffness coefficients, and mechanical mode amplitudes. So doing $\delta\psi_J$ and $\delta\zeta$ have been linked directly to the thermal contributions, modelled by Lindblad and non-Lindblad master equations, and to the shot noise forces. The mirror thermal noise has been expressed in the low frequency limit by the Levin’s formula. A corrective factor, for taking into account deviations of the cavity field from the fundamental mode, has been introduced.

The Drever–Pound and quadrant detector signals used for stabilizing respectively longitudinally and angularly the cavity, have been expressed in a form suitable to study the mutual coupling of these degrees of freedom in case of misalignment.

Emphasis has been put on the description of misalignment and mismatch of the input laser beam. To this end a vector approach has been adopted: the state of the input beam and the amplitudes of the excited cavity modes have been represented by vectors (\mathbf{v} and \mathbf{a} , respectively) and all the contributions to the cavity dynamic by a set of matrices. In this way, all the relevant quantities are given in form of algebraic products.

In particular, the optically-induced stiffness coefficients relative to the suspension modes have been expressed in the form $\mathbf{v}^\dagger \cdot \mathfrak{F} \cdot \mathbf{v}$, $\mathbf{v}^\dagger \cdot \mathfrak{T} \cdot \mathbf{v}$ with \mathfrak{F} , \mathfrak{T} matrices. It has been shown numerically that these coefficients may become very large in misaligned cavities close to unstable configurations.

The finite cavity round-trip time has been included in the model by introducing a delay operator. Consequently the cavity has been represented in the frequency domain by frequency dependent matrices containing stiffness coefficients.

The reported model simplifies notably in proximity of mechanical resonances. In particular the covariance matrix σ of two close in frequency vibrational modes has been expressed in terms of the stiffness coefficients and used for evaluating the system entanglement. This matrix also controls the squeezing degree of the output field.

The numerical examples refer to almost concentric cavities of length varying between 1 cm and 10 cm, spot size .2 cm and misalignment of .1 mrad.

APPENDIX A: FORCE, TORQUES AND STIFFNESS OPERATORS

$$\begin{aligned}\bar{\mathbf{F}}_0 &= J_p^2 \mathbf{G}_p^\dagger \cdot \mathbf{G}_p \\ \bar{\mathbf{T}}_{0,q} &= J_p^2 \mathbf{G}_p^\dagger \cdot \mathbf{X}_q \cdot \mathbf{G}_p\end{aligned}\quad (\text{A1})$$

Next, the stiffness operators $\tilde{\mathfrak{F}}, \tilde{\mathfrak{X}}_q$ are given by

$$\begin{aligned}\tilde{\mathfrak{F}} &= 2J_p^2 \Im \left\{ \tilde{\mathfrak{F}}_p \right\} \\ \tilde{\mathfrak{X}}_q &= 2J_p^2 \Im \left\{ \tilde{\mathfrak{X}}_{qp} \right\}\end{aligned}\quad (\text{A2})$$

with

$$\begin{aligned}\tilde{\mathfrak{F}}_p &= e^{-i\psi} R_p \mathbf{G}_p^\dagger \cdot \tilde{\mathbf{G}}_p \cdot \Phi \cdot \mathfrak{X} \cdot \mathbf{G}_p \\ \tilde{\mathfrak{X}}_{qp} &= e^{-i\psi} R_p \mathbf{G}_p^\dagger \cdot \mathbf{X}_q \cdot \tilde{\mathbf{G}}_p \cdot \Phi \cdot \mathfrak{X} \cdot \mathbf{G}_p\end{aligned}\quad (\text{A3})$$

while

$$\begin{aligned}\delta \tilde{\mathbf{F}}_{J,cav}^{DEF} &= 2J_p^2 \Im \left\{ \delta \tilde{\mathbf{F}}_{Jp,cav}^{DEF} \right\} \\ \delta \tilde{\mathbf{T}}_{Jq,cav}^{DEF} &= 2J_p^2 \Im \left\{ \delta \tilde{\mathbf{T}}_{Jqp,cav}^{DEF} \right\}\end{aligned}\quad (\text{A4})$$

with

$$\begin{aligned}\delta \tilde{\mathbf{F}}_{Jp,cav}^{DEF} &= e^{-i\psi} R_p \mathbf{G}_p^\dagger \cdot \tilde{\mathbf{G}}_p \cdot \Phi \cdot \delta \zeta_{J,cav}^L \cdot \mathbf{G}_p \\ \delta \tilde{\mathbf{T}}_{Jqp,cav}^{DEF} &= e^{-i\psi} R_p \mathbf{G}_p^\dagger \cdot \mathbf{X}_q \cdot \tilde{\mathbf{G}}_p \cdot \Phi \cdot \delta \zeta_J^L \cdot \mathbf{G}_p\end{aligned}\quad (\text{A5})$$

where $\delta \zeta_{J,cav}^L$ takes the Levin's form,

$$\delta \zeta_{J,cav}^L = e^{i\varpi\tau} \zeta_J^L \delta \zeta_J^L + e^{i\varpi\tau/2} \zeta_J^L \delta \zeta_J^L$$

Finally the action of the modes $J's'$ on the Js one is represented by the ensemble of matrices

$$\tilde{\mathbf{F}}_{JsJ's'}^{DEF} = 2J_p^2 \Im \left\{ \tilde{\mathbf{F}}_{pJsJ's'}^{DEF} \right\}\quad (\text{A6})$$

with

$$\tilde{\mathbf{F}}_{pJsJ's'}^{DEF} = e^{-i\psi} R_p \mathbf{G}_p^\dagger \cdot \zeta_{Js} \cdot \tilde{\mathbf{G}}_p \cdot \Phi \cdot \zeta_{J's'} \cdot \mathbf{G}_p\quad (\text{A7})$$

APPENDIX B: DREVER-POUND SIGNAL

$$\begin{aligned}\mathbf{I}^{DP} &= 2J_{p-k} J_p \Im \left\{ e^{i\varphi} \mathbf{G}_p^{OUT\dagger} \cdot \mathbf{G}_{p-k}^{OUT} \right\} \\ \tilde{\mathbf{J}}_{\pm}^{DP} &= 2J_{p\pm k} J_p \\ \Re \left\{ e^{-i(\psi \mp \varphi)} R_{p\pm k} \mathbf{G}_p^{OUT\dagger} \cdot \tilde{\mathbf{G}}_{p\pm k} \cdot \Phi \cdot \mathfrak{X} \cdot \mathbf{G}_{p\pm k} \right\} \\ \delta \tilde{\mathbf{I}}_{\pm}^{DP DEF} &= 2J_{p\pm k} J_p \\ \Re \left\{ e^{-i(\psi \mp \varphi)} R_{p\pm k} \mathbf{G}_p^{OUT\dagger} \cdot \tilde{\mathbf{G}}_{p\pm k} \cdot \Phi \cdot \delta \zeta_{1,cav}^{DEF} \cdot \mathbf{G}_{p\pm k} \right\} \\ \tilde{\mathbf{X}}_{\pm}^{DP SN} &= 2J_p \Re \left\{ \mathbf{v}_1^\dagger \cdot \mathbf{G}_p^{OUT\dagger} \cdot \delta \tilde{\mathbf{a}}_{p\pm k}^{OUT SN} \right\}\end{aligned}\quad (\text{B1})$$

APPENDIX C: SMALL MISALIGNMENT AND MISMATCH

Assuming $R = 1$ and $p = 0$ the ponderomotive force and torques read

$$\begin{aligned}\bar{F}_0 &= |G_{0(00,00)}|^2 \\ \bar{T}_{0,Jq} &= 2\text{Re} \left\{ G_{0(00,00)}^* G_{0(10,10)} v_{Jq} \right\}\end{aligned}$$

while the stiffness vectors reduce to

$$\begin{aligned}\tilde{\mathfrak{F}}_J &= \tilde{\mathfrak{F}}^{(0)} + 2\text{Re} \left\{ \tilde{\mathfrak{F}}_J^{(1)} \right\} \\ \tilde{\mathfrak{X}}_{Jq} &= \tilde{\mathfrak{X}}^{(0)} + 2\text{Re} \left\{ \tilde{\mathfrak{X}}_J^{(1)} \right\}\end{aligned}\quad (\text{C1})$$

with

$$\begin{aligned}\tilde{\mathfrak{F}}^{(0)} &= (\tilde{F}_\psi, 0, 0, 0) \\ \tilde{\mathfrak{X}}^{(0)} &= (0, \tilde{T}_X, \tilde{T}_Y, \tilde{T}_Z) \\ \tilde{\mathfrak{F}}_J^{(1)} &= (0, \tilde{F}_X v_{Jy}, \tilde{F}_X v_{Jz}, \tilde{F}_Y v_{Jy}, \tilde{F}_Y v_{Jz}) \\ \tilde{\mathfrak{X}}_J^{(1)} &= (\tilde{T}_\psi (v_{Jy} + v_{Jz}), 0, 0, 0)\end{aligned}\quad (\text{C2})$$

where

$$\begin{aligned}\tilde{F}_\psi &= 2\Im \left\{ e^{-i\psi - i2\phi_G} \tilde{G}_{0(00,00)} |G_{0(00,00)}|^2 \right\} \\ \tilde{T}_X &= 2\Im \left\{ e^{-i\psi - i4\phi_G} \tilde{G}_{0(10,10)} |G_{0(00,00)}|^2 \right\}\end{aligned}$$

Similar expression holds for \tilde{F}_X and \tilde{T}_ψ with $|G_{0(00,00)}|^2$ replaced by $G_{0(00,00)}^* G_{0(10,10)}$ while \tilde{F}_Y is similar to \tilde{F}_X with \Im replaced by \Re .

Analogously, for the Drever-Pound error signal

$$\begin{aligned}\bar{s}^{DP} &= \bar{s}^{(0)} \\ \tilde{s}^{DP} &= \tilde{s}^{(0)} + 2\text{Re} \left\{ \tilde{s}^{(1)} \right\} \\ \delta \tilde{s}_{cav}^{DP DEF} &= \delta \tilde{s}_{cav}^{(0) DEF} + 2\text{Re} \left\{ \delta \tilde{s}_{cav}^{(1) DEF} \right\}\end{aligned}\quad (\text{C3})$$

with

$$\begin{aligned}\bar{s}^{(0)} &= (\bar{s}_\psi, 0, 0, 0) \\ \tilde{s}^{(0)} &= (\tilde{s}_\psi, 0, 0, 0) \\ \tilde{s}^{(1)} &= (0, \tilde{s}_X v_{1y}, \tilde{s}_X v_{1z}, \tilde{s}_Y v_{1y}, \tilde{s}_Y v_{1z}) \\ \delta \tilde{s}^{(0) DEF} &= \tilde{s}_\psi \left(e^{i\omega\tau} \zeta_{1s(00,00)} \delta \zeta_{1s} + e^{i\omega\tau/2} \zeta_{2s(00,00)} \delta \zeta_{2s} \right) \\ \delta \tilde{s}^{(1) DEF} &= \tilde{s}_X^{(1)} \left(e^{i\omega\tau} (v_{1y} \zeta_{1s(00,01)} + \tilde{s}_X v_{1z} \zeta_{1s(00,10)}) \delta \zeta_{1s} \right. \\ &\quad \left. + e^{i\omega\tau/2} (v_{1y} \zeta_{2s(00,01)} + \tilde{s}_X v_{1z} \zeta_{2s(00,10)}) \delta \zeta_{2s} \right)\end{aligned}\quad (\text{C4})$$

where

$$\begin{aligned}\bar{s}_\psi &= J_{p+k} J_p 2\Im \left\{ e^{i\varphi} G_{p+k(00,00)}^{OUT*} G_{p(00,00)}^{OUT} \right\} \\ \tilde{s}_\psi &= 2J_{p+k} J_p \Re \left\{ e^{-i\psi - i2\phi_G} \right. \\ &\quad \left(e^{i\varphi} R_{p+k} G_{p(00,00)}^{OUT*} \tilde{G}_{p+k(00,00)}^{OUT} G_{p+k(00,00)}^{OUT} \right. \\ &\quad \left. \left. - e^{-i\varphi} R_p G_{p+k(00,00)}^{OUT*} \tilde{G}_{p(00,00)}^{OUT} G_{p(00,00)}^{OUT} \right) \right\}\end{aligned}\quad (\text{C5})$$

\tilde{s}_X is similar to \tilde{s}_ψ with $G_{p+k(00,00)}^{OUT}$, $G_{p(00,00)}^{OUT}$ replaced by $G_{p+k(10,10)}^{OUT}$, $G_{p(10,10)}^{OUT}$, while \tilde{s}_Y is similar to \tilde{s}_X with \Re replaced by \Im .

Finally the shot noise contribution reads

$$\tilde{X}^{DP SN} = \tilde{X}^{DP SN (0)} + \tilde{X}^{DP SN (1)}$$

where

$$\begin{aligned}\tilde{X}^{DP SN (0)} &= 2J_p \Re \left\{ G_{p(00,00)}^{OUT*} \left(\delta \tilde{a}_{p+k(00)}^{SN} - \delta \tilde{a}_{p-k(00)}^{SN} \right) \right\} \\ \tilde{X}^{DP SN (1)} &= 2\Re \left\{ G_{p(10,10)}^{OUT*} \left(\left(\delta \tilde{a}_{p+k(10)}^{SN} - \delta \tilde{a}_{p-k(10)}^{SN} \right) v_{1y}^* \right. \right. \\ &\quad \left. \left. + \left(\delta \tilde{a}_{p+k(01)}^{SN} - \delta \tilde{a}_{p-k(01)}^{SN} \right) v_{1z}^* \right) \right\}\end{aligned}$$

APPENDIX D: THERMAL AND SHOT-NOISE SOURCES

$$\begin{aligned}\tilde{\chi}_{J\psi}^{TH/SN} &= \tilde{\chi}_{J\psi} \tilde{X}_{J\psi}^{TH/SN} + \tilde{\chi}_{J\psi\theta z} \tilde{X}_{J\theta z}^{TH/SN} \\ &\quad + \delta_{1J} H^{DP} \mathcal{E}^2 \tilde{s}^{DP TH/SN} \\ \tilde{\chi}_{Jq}^{TH} &= \tilde{\chi}_{Jq} \tilde{X}_{Jq}^{TH} \\ \tilde{\chi}_{J\theta z}^{TH/SN} &= \tilde{\chi}_{J\theta z\psi} \tilde{X}_{J\psi}^{TH/SN} + \tilde{\chi}_{J\theta z} \tilde{X}_{J\theta z}^{TH/SN} \\ &\quad + \delta_{1J} H_z^{QD} \mathcal{E}^2 \tilde{s}_z^{QD TH/SN} \\ \tilde{\chi}_{J\theta y}^{TH} &= \tilde{\chi}_{J\theta y} \tilde{X}_{J\theta y}^{TH} + \delta_{1J} H_y^{QD} \mathcal{E}^2 \tilde{s}_y^{QD TH}\end{aligned}\quad (D1)$$

while for the mirror modes

$$\tilde{\chi}_{J_s}^{DEF TH/SN} = \chi_{J_s} \tilde{X}_{J_s}^{DEF TH/SN}$$

APPENDIX E: THERMAL NOISE CORRELATIONS

The correlations $\overline{\tilde{X}^{TH}(\varpi) \tilde{X}^{TH}(\varpi')} = C^{XX TH} \delta(\varpi + \varpi'), \dots$ of the thermal sources (39) and (41) for the Diosi master equation (see [12]) are given by

$$\begin{aligned}\tilde{C}^{XX TH} &= \frac{4k_B T}{\hbar\varpi_J} + \frac{|\varpi + i\gamma_J|^2}{\varpi_J^2} \frac{\hbar\varpi_J}{3k_B T} \\ &\quad + 2\frac{\varpi}{\varpi_J} \\ \tilde{C}^{YY TH} &= \frac{4k_B T}{\hbar\varpi_J} + \frac{\varpi_J^2}{\varpi^2} \frac{\hbar\varpi_J}{3k_B T} + 2\frac{\varpi}{\varpi_J} \\ \tilde{C}^{XY TH} &= \tilde{C}^{YX TH*}(\varpi) = \frac{4k_B T}{\hbar\varpi_J} \\ &\quad + \frac{\varpi + i\gamma_{J\lambda\hat{j}}}{\varpi} \frac{\hbar\varpi_J}{3k_B T} + \frac{\varpi_{J\lambda\hat{j}}}{\varpi} + \frac{\varpi + i\gamma_{J\lambda\hat{j}}}{\varpi_{J\lambda\hat{j}}}\end{aligned}\quad (E1)$$

while for the master equation of Ref. [14]

$$\begin{aligned}\tilde{C}^{XX TH} &= \tilde{C}_{GV}^{YY TH} = \tilde{C}_{GV}^{XY TH} \\ &= 2\frac{\varpi}{\varpi_J} \left(1 + \coth \left(\frac{\hbar\varpi}{2K_B T} \right) \right)\end{aligned}$$

On the other hand the commutators coincide

$$\overline{\left[\tilde{X}^{DEF TH}, \tilde{X}/\tilde{Y}^{DEF TH} \right]} = 4\frac{\varpi}{\varpi_J}\quad (E2)$$

APPENDIX F: SHOT NOISE CORRELATIONS

The Fourier transforms of the shot noise force and torque (27) are characterized by the correlations

$$\begin{aligned}\overline{\tilde{X}_{J_i}^{SN}(\varpi) \tilde{X}_{J_{i'}}^{SN}(\varpi')} \\ = \left(1 + \frac{t_2^2}{t_1^2} \right) \tilde{C}_{J_i J_{i'}}^{SN} \delta(\varpi + \varpi')\end{aligned}$$

where

$$\tilde{C}_{J_i J_{i'}}^{SN} = \mathbf{v}_J^\dagger \cdot \tilde{\mathbf{C}}_{ii'}^{SN} \cdot \mathbf{v}_{J'}$$

with

$$\tilde{\mathbf{C}}_{ii'}^{SN} = J_p^2 \mathbf{G}_p^* \cdot \mathbf{X}_i \cdot \left| \tilde{\mathbf{G}}_p \right|^2 \cdot \mathbf{X}_{i'} \cdot \mathbf{G}_p$$

and $i, i' = 1, 2, 3$. In particular, $\tilde{\mathbf{C}}_{J_i J_{i'}}^{SN} = \tilde{\mathbf{C}}_{J_{i'} J_i}^{SN \dagger}$. Analogously for $\tilde{X}_{J_s}^{DEF SN}$ (see (28)),

$$\begin{aligned}\overline{\tilde{X}_{J_s}^{DEF SN}(\varpi) \tilde{X}_{J_{s'}}^{DEF SN}(\varpi')} \\ = \left(1 + \frac{t_2^2}{t_1^2} \right) \tilde{C}_{J_s J_{s'}}^{DEF SN} \delta(\varpi + \varpi')\end{aligned}$$

where

$$\tilde{C}_{J_s J_{s'}}^{DEF SN} = \mathbf{v}_J^\dagger \cdot \tilde{\mathbf{C}}_{J_s J_{s'}}^{DEF SN} \cdot \mathbf{v}_{J'}\quad (F1)$$

with

$$\begin{aligned}\tilde{\mathbf{C}}_{J_s J_{s'}}^{DEF SN} &= J_p^2 \mathbf{G}_p^* \cdot \varsigma_{J_s} \cdot \left| \tilde{\mathbf{G}}_p \right|^2 \cdot \\ &\quad \cdot \varsigma_{J_{s'}} \cdot \mathbf{G}_p\end{aligned}\quad (F2)$$

In addition,

$$\begin{aligned}\overline{\left[\tilde{X}_{J_s}^{DEF SN}(\varpi), \tilde{X}_{J_{s'}}^{DEF SN}(\varpi') \right]} \\ = i2 \left(1 + \frac{t_2^2}{t_1^2} \right) \text{Im} \left\{ \tilde{C}_{J_s J_{s'}}^{DEF SN} \right\} \delta(\varpi + \varpi')\end{aligned}$$

[1] F. V. Kowalski, J. Hough, G. M. Ford, A. J. Munley, R. W. Drever, J. L. Hall and H. Ward. *Appl. Phys. B*, 31

97, (1983);

- [2] P. La Penna, A. Di Virgilio, M. Fiorentino, A. Porzio, S. Solimeno, *Opt. Commun.*, 162, 267 (1999); E. D'Ambrosio, *Phys. Rev. D* 67, 102004 (2003);
- [3] Bernardini et al. *Phys. Lett. A*, 243:187–194, (1998); G. Cella, V.S. Chickarmane, A. Di Virgilio, A. Gaddi, A. Vicerè *Phys. Letters A*, 266, 1 (2000); L. Bracci et al., *Class. Quant. Grav.*, 19:1675-1682 (2002); A. Di Virgilio et al., *Phys. Lett. A*, 316:1-9 (2003); —, *Phys. Lett. A*, 318:199-204 (2003); —, *Phys. Lett. A*, 322:1-9 (2004); —, *Class. Quant. Grav.*, 21:S1099-S1106 (2004); —, "Considerations on collected data with the Low Frequency Facility Experiment", *accepted for publication in J. Phys. Conf. Series*, (2005);
- [4] P. Fritschel, N. Mavalvala, D. Shoemaker, D. Sigg, M. Zucker, and G. Gonzales, *Appl. Opt.* 37, 6734 (1998);
- [5] A. Dorsel, J. D. McCullen, P. Meystre, E. Vignes, and H. Walter, *Phys. Rev. Letters* 51, 1550 (1983); A. Gozzini, F. Maccarrone, F. Mango, I. Longo, and S. Barbarino, *JOSAB* 2, 1841 (1985)
- [6] L. R. Miller, G. E. Moss and R. L. Forward. *Appl. Opt.*, 10:2495–2498, (1971); Z. Vager, A. Abramowich and M. Weksler. *J. Phys. E*, 19:182–188, (1986); J.-P. Richard, *Phys. Rev. D*, 46, 2309 (1992); H. J. Kimble, R. Lalezari, G. Rempe, R. J. Thompson, *Opt. Lett.* 17, 363 (1992).; N. Mio and K. Tsubono. *Appl. Opt.*, 34, 186 (1995).
- [7] Overviews of the different studies can be found on the different projects web sites: <http://www.ego-gw.it>; <http://www.ligo.caltech.edu>; <http://www.geo600.uni-hannover.de>; <http://tamago.mtk.nao.ac.jp>;
- [8] C. K. Law, *Phys. Rev. A* 51:2537 (1995);
- [9] A. F. Pace, M. J. Collett, and D. F. Walls, *Phys. Rev. A* 47:3173 (1993)
- [10] N. Deruelle and P. Tourrenc in *Gravitation, Geometry and Relativistic Physics*, Springer-Verlag, Berlin (1984); P. Tourrenc and N. Deruelle *Ann. Phys. (Paris)* 10, 241 (1985); J. M. Aguirregabiria and L. Bel *Phys. Rev. A* 36, 3768 (1987); L. Bel, J. L. Boulanger and N. Deruelle *Phys. Rev. A* 37, 2563 (1988); B. Meers and N. MacDonald *Phys. Rev. A* 40, 3754 (1989); S. Solimeno, F. Barone, C. de Lisio, L. Di Fiore, L. Milano and G. Russo, *Phys. Rev. A* 43, 6227 (1991);
- [11] C.W. Gardiner, "Handbook of Stochastic Methods", Springer, Berlin (1985); A. O. Caldeira and A. J. Leggett, *Physica*, A 121, 587 (1983); — *Phys. Rev. A*, 31, 1059 (1985); W. G. Unruh and W. H. Zurek, *Phys. Rev. D*, 140, 1071 (1989);
- [12] K. Jacobs, I. Tittoonen, H. M. Wiseman and S. Schiller, *Phys. Rev. A*, 60, 538 (1999); I. Tittoonen, G. Breitenbach, T. Kalkbrenner, T. Muller, R. Conradt, S. Schiller, E. Steinsland, N. Blanc, and N. F. de Rooij, *Phys. Rev. A* 59, 1038 (1999);
- [13] W. J. Munro and C.W. Gardiner, *Phys. Rev. A*, 53, 2633 (1996); S. Guntzmann and F. Haake, *Z. Phys B* 101, 263 (1996);
- [14] V. Giovannetti and D. Vitali, *Phys. Rev. A*, 63, 23812 (2001);
- [15] A. Barchielli, *Phys. Rev. A*, 34, 1642 (1986);
- [16] M. J. Collet and C. W. Gardiner, *Phys. Rev. A* 30, 1386 (1984); C. W. Gardiner and M. J. Collett *Phys. Rev. A* 31, 3761 (1985);
- [17] V. Braginsky and A. Manukin, *Sov. Phys. JETP-USSR* 25, 653-655 (1967); V. Braginsky and A. Manukin, *Measurement of weak forces in Physics Experiments*, (University of Chicago Press, 1977), pp. 25-39.
- [18] J. Sidles and D. Sigg *LIGO document no. LIGO-P03005*
- [19] V. B. Braginsky, S. E. Strigin and S. P. Vyatchanin *Phys. Lett. A* 287, 331 (2001); — 293, 228 (2002); — 305, 111 (2002) W. Kells, and E. D'Ambrosio *Phys. Lett. A* 299, 326 (2002); S. W. Cheddidiwy, Chunnong Zhao, Li Ju and D. G. Blair *Class. Quantum Grav.* 21, 1253 (2004)
- [20] V. B. Braginsky and F. Ya. Khalili, *Phys. Lett. A* 257, 241 (1999); Benjamin S. Sheard, et al. *Phys. Rev. A*, 69, 051801 (2004); H. Rokhsari et al., *Opt. Expr.*, 13, 5293 (2005); Thomas Corbitt et al., LIGO-P050045-00-R (http://www.ligo.org/pdf_public/P050045.pdf); A. Di Virgilio, et al. "Evidence of an optical spring" *in preparation*;
- [21] V. Giovannetti, S. Mancini and P. Tombesi, *Europhys. Lett.* 54, 559 (2001); S. Mancini, V. Giovannetti, D. Vitali and P. Tombesi, *Phys. Rev. Lett.* 88, 120401 (2002); S. Mancini, D. Vitali, V. Giovannetti, and P. Tombesi, *Eur. Phys. J D.* 22:417 (2003);
- [22] A. Heidmann and S. Reynaud, *Phys. Rev. A*, 50, 4237 (1994); C. Fabre, M. Pinard, S. Bourzeix, A. Heidmann, E. Giacobino, and S. Reynaud, *Phys. Rev. A*, 49, 1337 (1994); M. Pinard, C. Fabre, and A. Heidmann, *Phys. Rev. A*, 51, 2443 (1995); P.F. Cohadon, A. Heidmann, and M. Pinard, *Phys. Rev. Letters* 83, 3174 (1999); Y. Hadjar, P. F. Cohadon, C. G. Aminoff, M. Pinard, and A. Heidmann, *Europhys. Letters* 47, 545 (1999); M. Pinard, P. F. Cohadon, T. Briant, and A. Heidmann, *Phys. Rev. A* 63, 013808 (2000); J. M. Courty, A. Heidmann, and M. Pinard, *Phys. Rev. Letters*, Feb (2003); T. Corbitt, K. Goda, N. Mavalvala, E. Mikhailov, D. Ottaway, S. Whitcomb, Y. Chen, Caltech Seminar, March (2004);
- [23] P. R. Saulson. *Phys. Rev. D*, 2437 (1990); G. I. Gonzalez and P. R. Saulson, *J Acoustic Soc. Am.* 96, 207 (1994); Gillespie, A. and Raab, R., *Phys. Rev. D* 52, 577 (1995); F. Bondue and J.-Y. Vinet, *Phys. Lett. A* 198, 74 (1995); F. Bondue, P. Hello and J-Y Vinet, *Phys. Lett. A* 246, 227 (1998);
- [24] Y. Hadjar "High sensitivity optical measurement of mechanical Brownian motion of interferometric detector of Virgo gravitational wave PhD, LAL Orsay (1999)
- [25] K. Numata, M. Ando, K. Yamamoto, S. Otsuka and K. Tsubono, *Phys. Rev. Lett.* 91, 260602 (2003)
- [26] Yu. Levin, *Phys. Rev. D* 57, 659 (1998);
- [27] A. Vicerè Proc. Int. Summer School on Exp. Phys. of Gravitational Waves, World Scientific Publishing Co. Pte. Ltd., Singapore, (2000).